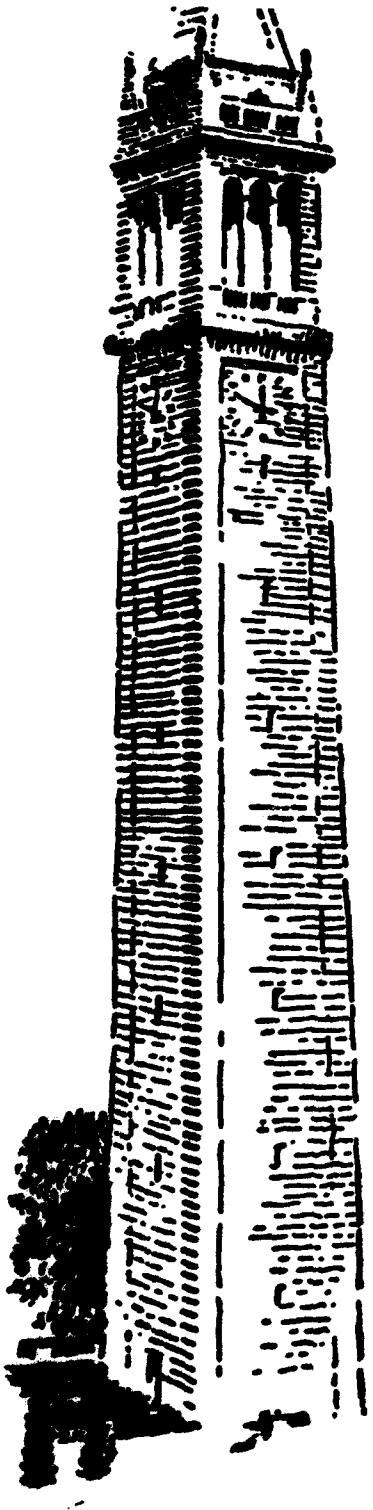

ANNUAL PROGRESS REPORT, FOR 1989
PLASMA THEORY AND SIMULATION GROUP

Professor C.K. Birdsall

January 1 to December 31, 1989

DOE Contract
DE-FG03-86ER53220 1/1/86 – 10/31/89
DE-FG03-90ER54079 10/31/89 – 2/28/93
ONR Contract N00014-85-K-0809
IR&D Grant from LLNL 8447605

ELECTRONICS RESEARCH LABORATORY
College of Engineering
University of California, Berkeley, CA 94720

SECURITY CLASSIFICATION OF THIS PAGE (When Data Entered)

REPORT DOCUMENTATION PAGE		READ INSTRUCTIONS BEFORE COMPLETING FORM
1. REPORT NUMBER	2. GOVT ACCESSION NO.	3. RECIPIENT'S CATALOG NUMBER
4. TITLE (and Subtitle) Annual Progress Report January 1, 1989 - December 31, 1989		5. TYPE OF REPORT & PERIOD COVERED Progress, 1/89 - 12/89 6. PERFORMING ORG. REPORT NUMBER
7. AUTHOR(s) Professor Charles K. Birdsall		8. CONTRACT OR GRANT NUMBER(s) ONR N00014-85-K-0809
9. PERFORMING ORGANIZATION NAME AND ADDRESS Electronics Research Laboratory University of California Berkeley, CA 94720		10. PROGRAM ELEMENT, PROJECT, TASK AREA & WORK UNIT NUMBERS Element No. 61153N, Project Task Area RRQ1-09-01, Work Unit No. NR 012-742
11. CONTROLLING OFFICE NAME AND ADDRESS ONR Physics Division Department of the Navy, ONR Arlington, VA 22217		12. REPORT DATE 13. NUMBER OF PAGES
14. MONITORING AGENCY NAME & ADDRESS(if different from Controlling Office)		15. SECURITY CLASS. (of this report) Unclassified 15a. DECLASSIFICATION/ DOWNGRADING SCHEDULE

16. DISTRIBUTION STATEMENT (of this Report)

Approved for public release; distribution unlimited

17. DISTRIBUTION STATEMENT (of the abstract entered in Block 20, if different from Report)

18. SUPPLEMENTARY NOTES

Our group uses theory and simulation as tools in order to increase the understanding of plasma instabilities, heating, transport, plasma-wall interactions, and large potentials in plasmas. We also work on the improvement of simulation both theoretically and practically.

19. KEY WORDS (Continue on reverse side if necessary and identify by block number)

Research in plasma theory and simulation, plasma-wall interactions, large potentials in plasmas, bounded plasmas.

20. ABSTRACT (Continue on reverse side if necessary and identify by block number)

This is a brief progress report, covering our research in general plasma theory and simulation, plasma-wall physics theory and simulation, and code development. Reports written in this period are included with this mailing. A publications list plus abstracts for two major meetings are included.

DD FORM 1 JAN 73 1473 EDITION OF 1 NOV 65 IS OBSOLETE

S/N 0102-LF-014-6601

SECURITY CLASSIFICATION OF THIS PAGE (When Data Entered)

ANNUAL PROGRESS REPORT
FROM
PLASMA THEORY AND SIMULATION GROUP

January 1 to December 31, 1989

Our research group uses both theory and simulation as tools in order to increase the understanding of instabilities, heating, transport, plasma-wall interactions, and large potentials in plasmas. We also work on the improvement of simulation, both theoretically and practically.

Our staff is:

Professor C.K. Birdsall *Principal Investigator*	191M	Cory Hall	643-6631
Dr. Ian Morey (until August) *Post-doctorate*	187M	Cory Hall	642-3477
Mr. Scott Parker	199MD	Cory Hall	642-1297
Mr. Richard Procassini	199MD	Cory Hall	642-1297
Mr. Vahid Vahedi	199MD	Cory Hall	642-1297
Mr. Julian Cummings	199MD	Cory Hall	642-1297
Mr. John Verboncoeur	199MD	Cory Hall	642-1297
Mr. Henry Heikkinen	199MD	Cory Hall	642-1297
Mr. Frank Tsung *Research Assistants(students)*	199MD	Cory Hall	642-1297
M. Virginia Alves Visitor (from Brazil, February on)			

Our advisers are:

Dr. Ilan Roth *Physicist, Space Science Lab, UCB*	304	SSL	642-1327
Dr. Bruce Cohen	L630	LLNL	422-9823
Dr. Alex Friedman	L630	LLNL	422-0827
Dr. A. Bruce Langdon *Physicists, Lawrence Livermore Natl. Lab*	L472	LLNL	422-5444

December 31, 1989

DOE Contracts:
DE-FG03-86ER53220 1/1/86 - 10/31/89
DE-FG03-90ER54079 10/31/89 - 2/28/93
ONR Contract N00014-85-K-0809
IR&D Support from LLNL 8447605

ELECTRONICS RESEARCH LABORATORY

University of California
Berkeley, CA 94720

ANNUAL PROGRESS REPORT
January 1 to December 31, 1989

Our research for 1989 has been widely reported, as given by the listing following, of 7 Journal Articles, 4 ERL Reports, 10 Talks, Conference Proceedings, and 8 Talks, Poster Papers.

Abstracts are attached for most of the talks; full papers for the Numerical Simulation Conference.

Sent along with this Report are reprints of the Journal Articles and the ERL Reports.

Our prior mode was to publish Quarterly Progress Reports; these then became Semi-Annual Reports, which ended in 1988. In 1989, we began publishing Annual Progress Reports. While QPR's were excellent exercises in reporting, they required an immense effort; in today's research climate, such effort is not available.

We trust that our reporting is still useful.

C.K. Birdsall
Principal Investigator

Publications for 1989

Journal Articles

W.S. Lawson, "Particle Simulation of Bounded 1D Plasma Systems," *J. Comp. Physics*, **80** (2), February 1989, pp. 253-276.

K. Theilhaber and C.K. Birdsall, "Kelvin-Helmholtz Vortex Formation and Particle Transport in a Cross-Field Plasma Sheath," *Phys. Rev. Lett.*, **62**, pp. 772-775, February 13, 1989.

B.I. Cohen, A.B. Langdon, D.W. Hewett (all at LLNL) and R.J. Procassini (here), "Performance and Optimization of Direct Implicit Particle Simulation", *J. Comp. Phys.*, **81**, pp 151-168, March 1989

William S. Lawson, "The Pierce Diode with an External Circuit. I. Oscillations About Nonuniform Equilibria," *Phys. Fluids B*, **1**, July 1989, pp 1483-1492.

William S. Lawson, "The Pierce Diode with an External Circuit. II. Chaotic Behavior," *Phys. Fluids B*, 1, July 1989, pp. 1493-1501.

K. Theilhaber and C.K. Birdsall, "Kelvin-Helmholtz Vortex Formation and Particle Transport in a Cross-Field Sheath I: Transient Behavior," *Phys. Fluids B*, 1, pp. 2244-2259, November 1989.

K. Theilhaber and C.K. Birdsall, "Kelvin-Helmholtz Vortex Formation and Particle Transport in a Cross-Field Sheath II: Steady State," *Phys. Fluids B*, 1, pp2260-2272, November 1989.

ERL Reports

J. Verboncoeur, "ES1 Reference Manual" (which is distributed with our PC disk, which is not included here - but free for the asking)

M.J. Gerver, S.E. Parker, and K. Theilhaber, "Analytic Solutions and Particle Simulations of Cross-Field Plasma Sheaths," Memo No. UCB/ERL M89/114, August 30, 1989.

I.J. Morey, and C.K. Birdsall, "Traveling-Wave-Tube Simulation: The IBC Code," Memo No. UCB/ERL M89/116, September 26, 1989.

S.E. Parker, and C.K. Birdsall, "Numerical Error in Electron Orbits with Large $\omega_{ce}\Delta t$," Memo No. UCB/ERL M89/136, December 20, 1989.

Talks, Conference Proceedings

At *Sherwood Theory Conference*, San Antonio, Texas, April 3-5, 1989:

W.S. Lawson and C.K. Birdsall, "Simulation of RF driven plasma edge."

S.E. Parker, C.K. Birdsall, A. Friedman, S.L. Ray, "Bounded multi-scale particle simulation: The sheath problem."

At *13th Conference on Numerical Simulation of Plasmas*, Santa Fe, NM, September 17-20, 1989

J.P. Verboncoeur, V.. Vahedi, "WinGraphics: An Optimized Windowing Environment for Interactive Real-Time Simulations."

I.J. Morey, J.P. Verboncoeur, and V. Vahedi, "Bounded Plasma Device Simulation with PDW1, Including: External RLC Circuit, DC and RF Drive, and Collisional Processes."

I.J. Morey, and C.K. Birdsall, "The Traveling–Wave–Tube Code IBC."

M.V. Alves, V. Vahedi, and C.K. Birdsall, "PDC1: One-Dimensional Radial Code for a Cylindrical Plasma Device with an External RLC Circuit."

S.E. Parker, A. Friedman, S.L. Ray, and C.K. Birdsall, "Multi–Scale Particle Simulation of Bounded Plasmas."

S.E. Parker, "A Particle–In–Cell Method for Modeling Small Angle Coulomb Collisions in Plasmas."

R.J. Procassini, C K. Birdsall, B.I. Cohen, and Y. Matsuda, "Comparison of Particle–In–Cell and Fokker–Planck Methods as Applied to the Modeling of Auxiliary–Heated Mirror Plasmas."

Talks, Poster Papers

At *APS/Gaseous Electronics Conference Annual Meeting*, Palo Alto, CA, October 17-20, 1989

I.J. Morey, V. Vahedi, J.P. Verboncoeur, and M.A. Lieberman, "Particle Simulation Code for Modeling Processing Plasmas."

M.V. Alves, V. Vahedi, and C.K. Birdsall, "Cylindrical Simulations for RF Discharges and Plasma Immersion Ion Implantation."

At *APS/Division of Plasma Physics Annual Meeting*, Anaheim, November 13-17, 1989.

R.J. Procassini, C.K. Birdsall, and B.I. Cohen, "Particle Simulations of a Low-Recycling Divertor Scrape–Off Layer."

C.K. Birdsall, R.J. Procassini, and B.I. Cohen, "Particle Simulations of a High–Recycling Divertor Scrape–Off Layer."

R.J. Procassini, B.I. Cohen, Y. Matsuda, and C.K. Birdsall, "Modeling of Auxiliary–Heated Mirror Plasmas: A Comparison of Particle–In–Cell and Fokker–Planck Methods."

S.E. Parker, and R.J. Procassini, "Large Space and Time Scale Particle Simulation of Bounded Plasmas with a 'Logical Sheath'."

M.V. Alves, V. Vahedi, and C.K. Birdsall, "RF Plasma Processes in Cylindrical Models and Plasma Immersion Ion Implantation."

I.J. Morey, V. Vahedi, and J. Verboncoeur, "Particle Simulation Code for Modeling Processing Plasmas."

Sherwood Theory Conference, San Antonio, Texas, April 3-5, 1989

Sherwood Theory Meeting
San Antonio, Texas
April 3-5, 1989

Simulation of RF Driven Plasma Edge*

W. S. Lawson and C. K. Birdsall

Courant Institute of Mathematical Sciences
New York University
New York, NY 10012
and
Electronics Research Laboratory
University of California
Berkeley, CA 94720

Electrostatic computer simulations of a plasma edge driven by an RF electric field in a gap between two conductors (Faraday shields) will be presented. Results show that both the ion flux and the ion impact energies are roughly proportional to the applied power. Both the flux and average impact energy are strong functions of the drive frequency for the wide range of frequencies used, but may vary little over the narrower range of frequencies used in experiments. Ion heating occurs over the entire simulation region implying that waves (Ion Bernstein waves) are directly excited at the antenna. Direct observation of these waves will be attempted, and the results will be presented.

*This research was supported by U. S. Department of Energy grants no. DE-FG02-86ER53223 and no. DE-FG03-86ER53220.

Bounded Multi-Scale Particle Simulation: The Sheath Problem

S. E. Parker and C. K. Birdsall

Electronics Research Laboratory, Univ. of California, Berkeley

A. Friedman and S. L. Ray

Lawrence Livermore National Laboratory, Univ. of California, Livermore

We are using the multi-scale [1] technique to model bounded systems. Certain bounded systems are a naturally suited for the multi-scale method because the boundary layer (or sheath) that forms at the wall, which is usually a short spatial ($\sim \lambda_{De}$) and time scale ($\sim \omega_{pe}$) structure, can signif..antly effect the bulk plasma behavior. One goal is to understand the interaction between the bulk plasma and the sheath. If the relevant short time scale physics is local to a few (or one) spatial regions, then one can take advantage of this by advancing particles with variable Δt depending on position, hence reducing computing time. The unmagnetized sheath problem is such a case.

The model is a one dimensional bounded slab with kinetic ions and electrons. We start with a collisionless and unmagnetized system for simplicity. The right boundary is a conducting wall that absorbs all particles that come in contact with it. The left boundary is a symmetry point, where the particles are reflected. We allow a specified initial distribution: $f(x, v, t = 0)$, and a distributed source: $s(x, v, t)$.

To test the numerics of both the multi-scale method and boundary conditions we are using the following test problem: a cutoff Maxwellian distribution for the electrons and fixed (or infinitely massive) ions. The system has an analytic solution, so the run may be started from equilibrium. This gives us a benchmark to compare against and tests the fast time scale electron sheath dynamics. Initial results using variable Δt (with ratio of smallest to largest of 1:32) will be given. In the future, we intend to use the more general model to study time dependent sheath problems, such as a shock front interaction with the boundary.

[1] "Particle-In-Cell Plasma Simulation with a Wide Range of Space and Time Scales", A. Friedman, S.L. Ray, C.K. Birdsall, and S.E. Parker, Proc. 12th Conf. on Numerical Simulation of Plasmas, APS, San Francisco, Sept. 1988.

APS/Division of Plasma Physics Annual Meeting, Anaheim, CA, November 13-17, 1989

Particle Simulations of a Low-Recycling Divertor Scrape-Off Layer : R. Procassini, C. Birdsall, *University of California, Berkeley*; B. Cohen, *Lawrence Livermore National Laboratory*—The effect of Coulomb collisionality on the transport of particles and energy to a low-recycling divertor plate through the scrape-off layer (SOL) in a tokamak is studied using a fully-kinetic, self-consistent particle-in-cell (PIC) model. The two species (electron and ion) PIC code features a Monte Carlo binary-particle collision model which conserves the momentum and kinetic energy of the interacting particles. The full-range of Coulomb collisional processes (e-e, e-i and i-i) are included. The dependence of the presheath and collector sheath potential drops, plasma temperature, flow velocity and parallel heat flux on the collisionality is discussed. The "collisional" presheath drop, electron temperature at the plate, and collector sheath drop increase with collisionality. The electron temperature at the plate is much smaller than the source temperature, due to the loss of electrons over the collector sheath potential barrier. The electron heat flux, which is the main channel for energy transport along the field lines in the SOL, is reduced relative to the "free-streaming" heat flux $q_{fs} \equiv n_e v_{te} k T_e$, for finite (non-zero) values of the mean-free path $\lambda \equiv v_{te}/\nu_{coll}$.

*This work supported by the U.S. DOE under contract W-7405-Eng-48.

Particle Simulations of a High-Recycling Divertor Scrape-Off Layer : C. Birdsall, R. Procassini, *University of California, Berkeley*; B. Cohen, *Lawrence Livermore National Laboratory*—The effect of neutral/charged particle interactions on the transport of particles and energy to a high-recycling divertor plate through the scrape-off layer (SOL) in a tokamak is studied using a fully-kinetic, self-consistent particle-in-cell (PIC) model. In addition to a Monte Carlo binary-particle Coulomb-collision model, the basic electrostatic particle code also simulates the charge-exchange and impact-ionization processes which occur between plasma particles and recycled neutral particles in the vicinity of the divertor plate. (The neutral particle density profile is specified by the user, hence the neutral particles are not handled in a self-consistent manner). These atomic physics models may also be used as a source of sputtered impurity particles, which can then be followed by the code as a second ionic species. The dependence of the presheath and collector sheath potential drops, plasma temperature, flow velocity and parallel heat flux on the ratio of the charge-exchange/ionization rate to the Coulomb collision frequency is discussed. Comparison is made to other high-recycling divertor models.

*This work supported by the U.S. DOE under contract W-7405-Eng-48.

APS/Division of Plasma Physics Annual Meeting
Anaheim, CA, November 13-17, 1989

Modeling of Auxiliary-Heated Mirror Plasmas: A Comparison of Particle-In-Cell and Fokker-Planck Methods * J. PROCASSINI, B. COHEN, Y. MATSUDA, *Lawrence Livermore National Laboratory*; C. BIRDSALL, *University of California, Berkeley*—The transport and confinement of charged particles in an auxiliary-heated mirror plasma is modeled via a bounce-averaged Fokker-Planck (F-P) code and a direct-implicit particle-in-cell (PIC) code. The test case studied is that of a tandem mirror end plug plasma which is heated by the injection of fundamental and second harmonic ECRH wave energy. This test case determines the confinement and transport of electrons *only*, with the ions modeled as scattering sites. Both electron-electron and electron-ion collisions are included. The magnetic and electrostatic fields are prescribed quantities. Each code employs a relativistic description of the electron dynamics in one spatial dimension. The modeling comparison is divided into three sections: *i)* Benchmarking the physics results from the PIC code against those from the F-P code; *ii)* A computational cost analysis of each code; *iii)* A discussion of the advantages and disadvantages of each code, including a comparison of the effort involved in setting up each input deck.

*This work supported by the U S. DOE under contract W-7405-Eng-48.

Large space and time scale particle simulation of bounded plasmas with a "Logical Sheath" * S. E. PARKER AND R. PROCASSINI, *University of California, Berkeley*—When studying plasma flow to a conducting, absorbing plate, the sheath can affect the relevant physics. The sheath is a small space ($\sim \lambda_{De}$) and time ($\sim \omega_{pe}^{-1}$) scale structure. Hence, to include boundary effects in a particle simulation ordinarily one must resolve these small time and space scales. Fortunately, the Direct Implicit method has relaxed the $\omega_p \Delta t$ restraint for stability, but is not accurate at large $\omega_{pe}\Delta t$ for bounded simulations in which one wants to retain the sheath dynamics. We propose an alternative to resolving the sheath by implementing what we call the "logical sheath". We absorb ions and reflect electrons sequentially to maintain zero net current to the wall. The sheath drop is retained through the cutoff velocity of the electrons. Small time and space scale resolution is not necessary. We have already used the logical sheath in explicit simulations of a Q-machine. We plan to show implicit results with large $\omega_{pe}\Delta t$. By implementing the logical sheath, we plan to study kinetic effects in the divertor region of a tokamak.

*This work supported by DoE contract No. DE-FG03-86ER53220 and ONR contract N00014-85-K-0809.

Particle Simulation Code for Modeling Processing Plasmas * LJ. MOREY, V. VAHEDI AND J. VERBONCOEUR, *University of California, Berkeley*—The bounded plasma particle simulation code PDW1[1] has been modified to run interactively on a PC. A collision model has been added which can be used to simulate elastic, excitation, ionization and charge exchange collisions. The code already had models of external circuits and plasma sources, so a number of different processing plasmas can now be simulated. This includes RF and DC discharges and plasma immersion ion implantation devices. RF discharge simulations have shown rectification of the plasma potential, ions responding to the average potential, sheath heating and joule heating. Both voltage and current driven RF discharges have been examined, and differences have been observed between the harmonic content of the potential. Ion velocity distributions at the boundaries exhibit features due to charge exchange and ionization within the sheath regions. The code has excellent graphics and the many diagnostics are displayed in a window format, accessed using a menu system.

*This work supported in part by DOE contract DE-FG03-86ER53220 and ONR contract N00014-85-K-0809

[1]W.S. Lawson, J. Comp. Phys. 80, 253 (1989).

RF Plasma Processes in Cylindrical Models and Plasma Immersion Ion Implantation * M. V. ALVES †, V. VAHEDI AND C. K. BIRDSALL, *ERL, University of California, Berkeley*—

Spherical and cylindrical many-particle models are being used to simulate RF discharges in which the RF powered and the grounded electrodes have different areas. These also model plasma immersion ion implantation, where a target is pulsed negatively. PDC1, is a 1D radial, electrostatic code simulating a plasma contained between concentric cylinders coupled to an external RLC circuit and an RF source. Collisions with neutral particles are included as in PDW1[1] so that weakly ionized discharges can be simulated. The self-bias voltage (producing the ion bombarding energy) at the powered electrode is measured and compared with theory.[2] Pulsed plasma immersion ion implantation will also be described.

*This work supported in part by DOE contract DE-FG03-86ER53220 and ONR contract N00014-85-K-0809

†On leave from INPE - S. J. Campos - SP - Brazil

[1]L J. Morey, V. Vahedi, J. P. Verboncoeur, to be presented at this conference.

[2]M. A. Lieberman, J. Appl. Phys. 65, 4186 (1989).

ANNUAL PROGRESS REPORT

January 1, 1989 - December 31, 1989

The reports following are the full papers from the 13th Conference on Numerical Simulation of Plasmas which took place in Santa Fe, New Mexico, September 17 – 20, 1989.

WinGraphics: AN OPTIMIZED WINDOWING ENVIRONMENT FOR INTERACTIVE REAL-TIME SIMULATIONS

John P. Verboncoeur and Vahid Vahedi
Plasma Theory and Simulation Group
Electronics Research Laboratory
University of California
Berkeley, CA 94720

We have developed a customized windowing environment, WinGraphics, which provides particle simulation codes with an interactive user interface. The environment supports real-time animation of the simulation, displaying multiple diagnostics as they evolve in time. In addition, keyboard and printer (PostScript and dot matrix) support is prov.ded. The simulation codes are structured as shown in figure 1.

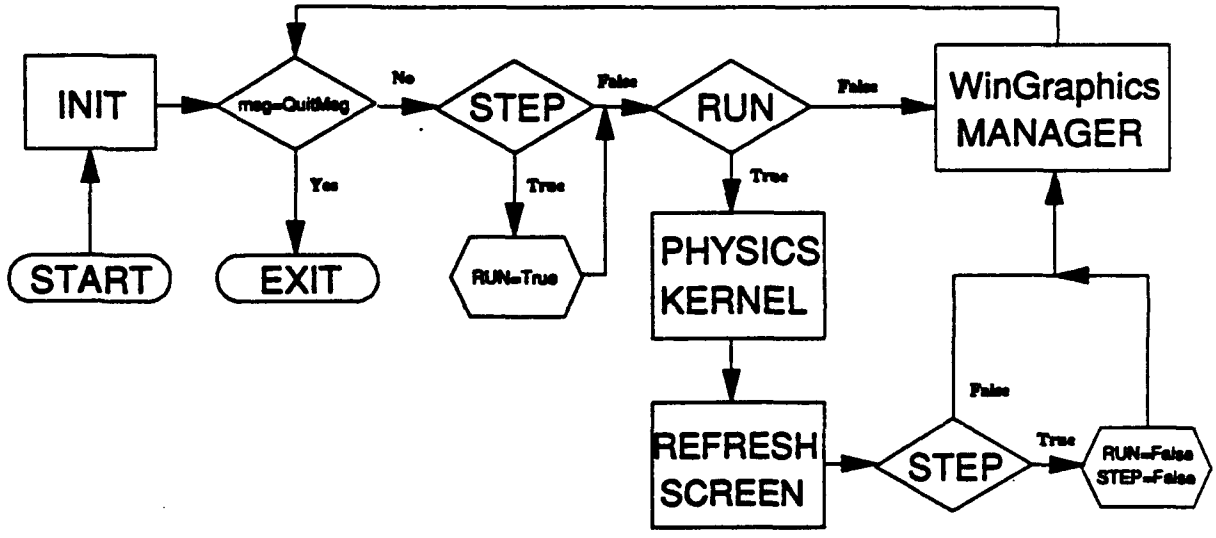

FIGURE 1. Schematic representation of the interaction between WinGraphics and the physics kernel.

The physics kernel is portable to any machine supporting standard C. The INIT module scans the input file containing the physical parameters of the problem and initializes the diagnostic windows. INIT also sets up memory for array storage. The environment provides hooks for the physics kernel to run continuously (there is no time limit - the code can run indefinitely) or step through individual timesteps. The screen is refreshed each timestep, and all user requests are processed by the WinGraphics MANAGER. When the simulation is in the running state, the MANAGER is invoked at each time step (if not running the MANAGER is constantly invoked) to check the keyboard buffer for the user's requests (messages). Pending messages are translated and dispatched by the MANAGER until the user requests QUIT.

The WinGraphics environment provides menus (as shown in figure 2), messages, prompts, and dialog boxes as well as keyboard support for navigating the above. These facilities allow interactive control of both the simulation and the output of the simulation.

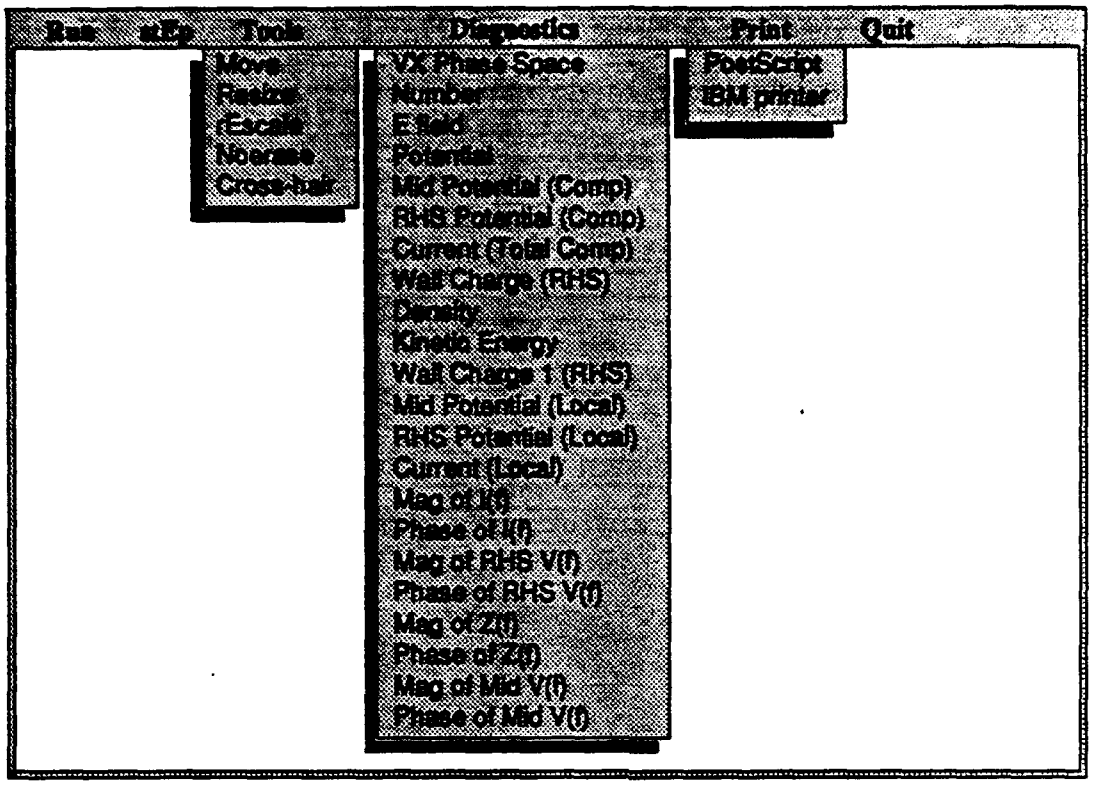

Figure 2. The WinGraphics menus for PDW1 [1].

WinGraphics controls the video display by managing each window as an object with the following attributes:

- Labels for each axis.
- The coordinates of the outer window frame and the client area.
- Scales for the x- and y-axes. These quantities are useful for normalized codes where values must be converted to some units before plotting.
- Maximum and minimum x and y coordinates of the plot.
- State of the object. The environment checks the state to determine if the window is on/off, if it was previously on, the type of plot(s) the window contains (semilog, linear, or scatter), if the window is overlapping other windows, and if it is currently/previously being autorescaled[1]. The state is used to minimize redrawing; objects which have not changed since the last screen update are not redrawn.

---

1. *Autorescale*: a process of scanning the x and y arrays for the maximum and minimum values. An autorescaled plot fills the entire client area of its window, and causes the axis labels to be recalculated each time they change.

- Linked list of curves to plot. The contents of the linked list include the number of points, pointers to the arrays, and the color of the curve. This enables windows to display multiple curves using the same axes.

By manipulating the above characteristics interactively, windows can be opened, closed, moved to a new location on the screen, made smaller or larger in two dimensions, and overlapped. In addition, WinGraphics provides an interactive crosshair with which the user can point to any location on the screen and display the coordinates of that point in the units of the plot containing the point.

WinGraphics provides management of the segmented Intel 80x86 memory by allocating only the required space for arrays and structures. Near arrays (addressed using the DS segment register and a 16-bit offset) are used for performance-critical variables, while far arrays (addressed with a 16-bit segment and a 16-bit address) are used for large arrays which cannot fit in the 64kB near heap of the 80x86.

Since the code can run for an indefinite number of timesteps, arrays which accumulate some physical quantity in time must be managed. The histories are combed when the array limit is reached, retaining only every *nth* value. This leads to loss of temporal resolution as the simulation is advanced in time. To retain local temporal resolution, local arrays are used which contain data for contiguous timesteps.

The codes currently running in the WinGraphics environment include ES1 (Electrostatic 1 Dimensional Periodic Plasma simulation) [2], PDW1 (Plasma Device Workshop 1 Dimensional Cartesian bounded simulation) [1], and PDC1 (the cylindrical counterpart of PDW1) [3].

Figure 3 shows a sample PostScript output of WinGraphics for ES1 displaying the variation of potential, $\phi(x)$ (left), and the time history of electrostatic field energy (right) for Landau damping with 8192 particles.

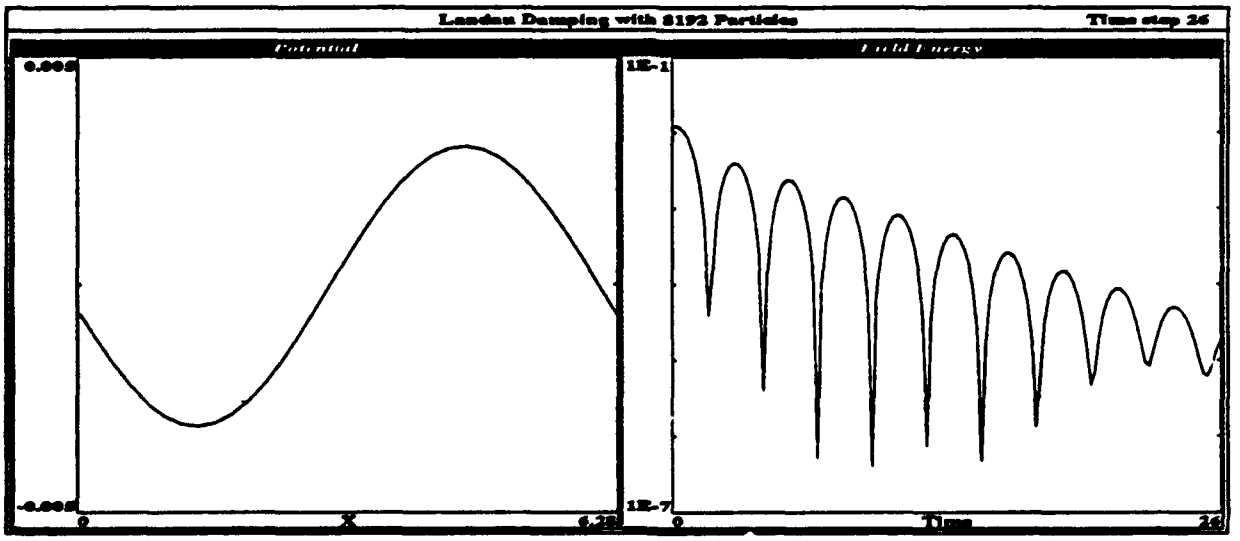

Figure 3. PostScript output of WinGraphics for ES1.

As a performance comparison of the codes, we use ES1 running a Landau damping simulation with 16000 electrons. The results of the comparison are shown below. The Cray values are given using the NMFECC Cray computers using the vectorized FORTRAN version of the code due to A. B. Langdon (LLNL).

computer	clock speed (MHz)	μsec per particle per push
IBM AT	6	1038
IBM PS/2 Model 80	16	183
Dell 310	20 + memory cache	118
Cray I	vectorized	1.8
Cray II	vectorized	1.4

From this information, we can extrapolate for new hardware. For example, an 80386/80387 running at 33 MHz with sufficiently fast memory should perform at 71 μsec per particle per push, an 80486 at 33 MHz should perform at 24 μsec per particle per push, and an 80486 running at 50 MHz should result in performance of 16 μsec per particle per push.

Clearly we are rapidly approaching the performance needed to run two dimensional codes on PC's. Note that as the number of dimensions increases, the relative computational cost of the field solve increases, so one cannot directly extrapolate from the 1D particle pushes. Given sufficient memory, it is estimated that a minimum speed of 40 μsec per particle per push (25,000 particles per second) is required to run a 2D simulation in real time. Memory requirements vary widely depending on the problem, but a good minimum estimate is 800k bytes (500k for particle quantities of 25,000 particles, 120k for quantities on a 100x100 grid, etc.)

ACKNOWLEDGEMENTS

Work supported in part by DOE Contract DE-FG03-86ER53220 and ONR Contract N00014-85-K-0809.
Development was done on IBM PC-AT's under DACE grant and on IBM PS/2 model 80 under *IBM Courseware Program*, for which we are most grateful.

---

[1] W. L. Lawson, *PDW1 USER'S MANUAL*, ERL Memorandum UCB/ERL M84/37 (1984).
W. L. Lawson, *J. Comp. Phys.* 80, 253 (1989).
I. J. Morey, J. P. Verboncoeur, V. Vahedi, to be presented at this conference (1989).

[2] C. K. Birdsall and A. B. Langdon, *Plasma Physics via Computer Simulation*, McGraw-Hill (1985).

[3] M. V. Alves, V. Vahedi, C. K. Birdsall to be presented at this conference (1989).

BOUNDED PLASMA DEVICE SIMULATION WITH PDW1, INCLUDING: EXTERNAL RLC CIRCUIT, DC AND RF DRIVE, AND COLLISIONAL PROCESSES.

Ian J. Morey, John P. Verboncoeur, and Vahid Vahedi
Plasma Theory and Simulation Group
Electronics Research Laboratory
University of California
Berkeley, CA 94720

PDW1 (Plasma Device Workshop 1-dimensional), running in the WinGraphics environment [1], is a versatile many-particle bounded plasma simulation code used to study diverse plasma and boundary conditions. The boundaries are connected through an external RLC circuit with time dependent voltage/current sources. Having a versatile input deck is an efficient way of specifiying plasma parameters to the code without recompiling. In PDW1, input deck parameters are given in MKS units. The list includes:

plasma variables:	number of species, characteristics of each species and background charge and current densities
device variables:	electrode separation, electrode area and background ε
circuit variables:	R, L, C, $V(t)$ and $I(t)$
electrode variables:	absorption, secondary emission and plasma sources
collision variables:	neutral pressure, elastic, excitation and ionization collisions
numerical variables:	Δt, Δx, number of cells, charge per computer particle and FFT period.

PDW1 employs four distinct circuit solvers to handle the full range of external circuit parameters. For the general series RLC circuit with voltage source, a 2nd order backward Euler is used. For $C \rightarrow 0$, the external circuit becomes an open circuit, and external parameters are ignored. For $C \rightarrow \infty$ and $R=L=0$, external potentials are applied directly across the plasma region. The final case is an ideal current source, which drives the specified current from one plate to the other (external circuit parameters do not affect an ideal current source).

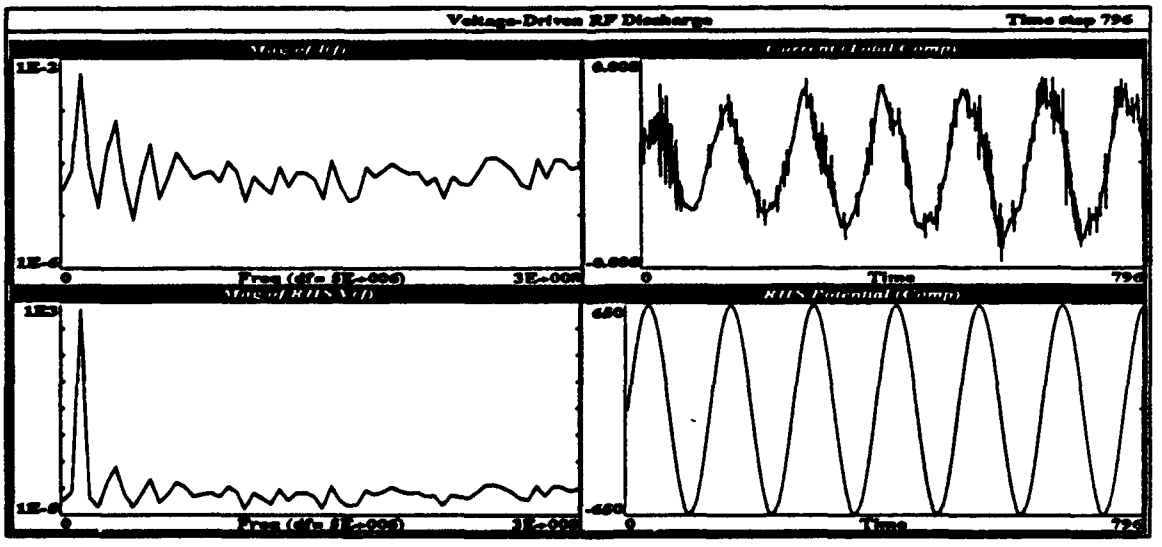

Figure 1. Time and frequency responses of voltage and current signals in an RF discharge.

FFT routines are used to obtain the frequency response of any signal accumulated in time. The quantities currently transformed include the driven wall potential, the potential at the middle of the system and the current. The total impedance, $Z(f)$, of the plasma region is calculated in the frequency domain as the ratio of $V(f)$ to $I(f)$. An example is shown in figure 1. for an RF discharge.

Collisions with neutral particles have been included in PDW1 so partially ionized discharges can be simulated. The present model can be used for elastic, inelastic and ionizing electron-neutral collisions, and can be extended to charge-exchange ion-neutral collisions. The full 3-D character of a collision is modelled with just two velocity components, parallel and perpendicular to the spatial dimension of the simulation.

The neutrals are assumed to be uniformly distributed between the boundaries with a constant density. The probability, P_m, that the m-*th* electron has a collision with a neutral is given by

$$P_m = 1 - \exp(-n\sigma_T(E_m)v_m\Delta t) \tag{1}$$

where n is neutral density, σ_T is the total cross-section (the sum of cross-sections for elastic, excitation and ionizing collisions) and v_m is the velocity of the m-*th* electron. Laboratory cross-sections are entered into arrays at the start of the run. A collision occurs if a random number $R(\ R \in [0,1])$ is less than P_m. Another random number is then used to determine what type of collision has occurred, based upon the following:

$$R \le \sigma_{el}(E)/\sigma_T(E) \qquad :elastic$$

$$\sigma_{el}(E)/\sigma_T(E) < R \le (\sigma_{el}(E) + \sigma_{ex}(E))/\sigma_T(E) \qquad :excitation$$

$$(\sigma_{el}(E) + \sigma_{ex}(E))/\sigma_T(E) < R \qquad :ionization$$

Once the type of collision is determined, the energy of the scattered electron is obtained. Energy is unchanged for elastic collisions, while excitation energy is lost during excitation collisions. During an ionizing collision the energy is divided between the two electrons using a differential ionization cross-section of the form:

$$S(E,T) = \frac{A(E)}{T^2 + B^2(E)} \tag{2}$$

where E is the incident electron energy, T is the scattered electron energy, and A and B are general functions of E. This is a simplified form of the cross-section used by Peterson and Allen [2].

Lastly, the directions of the scattered and ejected electrons are obtained by using the same differential cross-section to determine the scattering angle after all collisions, which has been taken from Den Hartog *et al* [3], and has the form

$$\frac{\sigma(T,\chi)}{\sigma(T)} = \frac{T}{4\pi(1 + T\sin^2(\chi/2))\ln(1+T)} \tag{3}$$

where χ is the angle between the incident and scattered velocities.

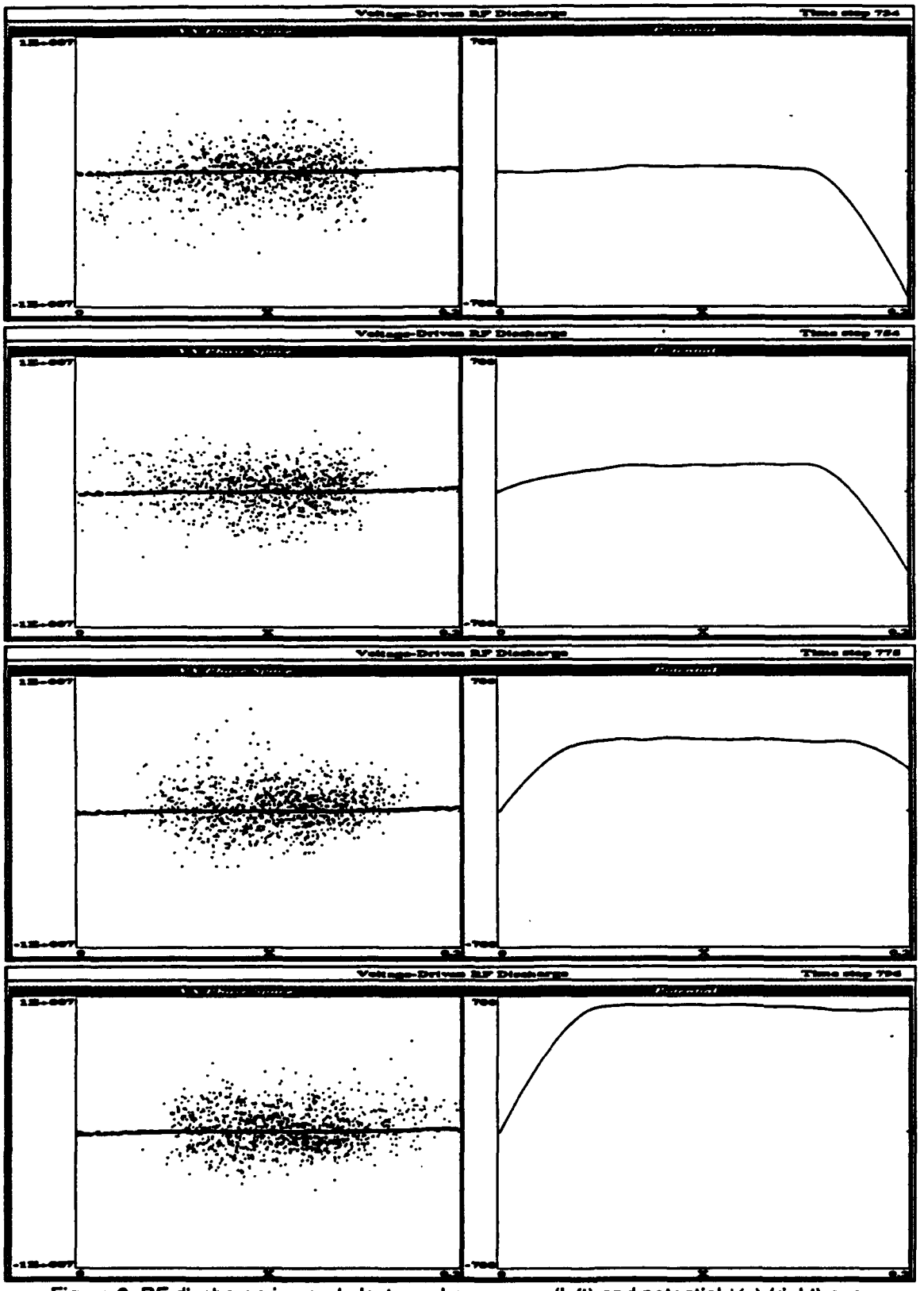

Figure 2. RF discharge ion and electron phase space (left) and potential $\phi(x)$ (right) over one half-cycle with right wall driven at 10 *MHz*, $\Delta t = 1\eta$ sec

Figure 2 shows a sample run of PDW1 for an RF-driven discharge over one half-cycle, displaying the velocity phase space (velocity versus position for each particle), and the variation of potential, $\phi(x)$, from wall to wall.

The left-hand plot in figure 3 shows the velocity phase space in expanded scale, as the ions accelerate out to the walls from the bulk plasma due to the presence of an average positive potential, as seen in the right-hand plot, in the middle of the system.

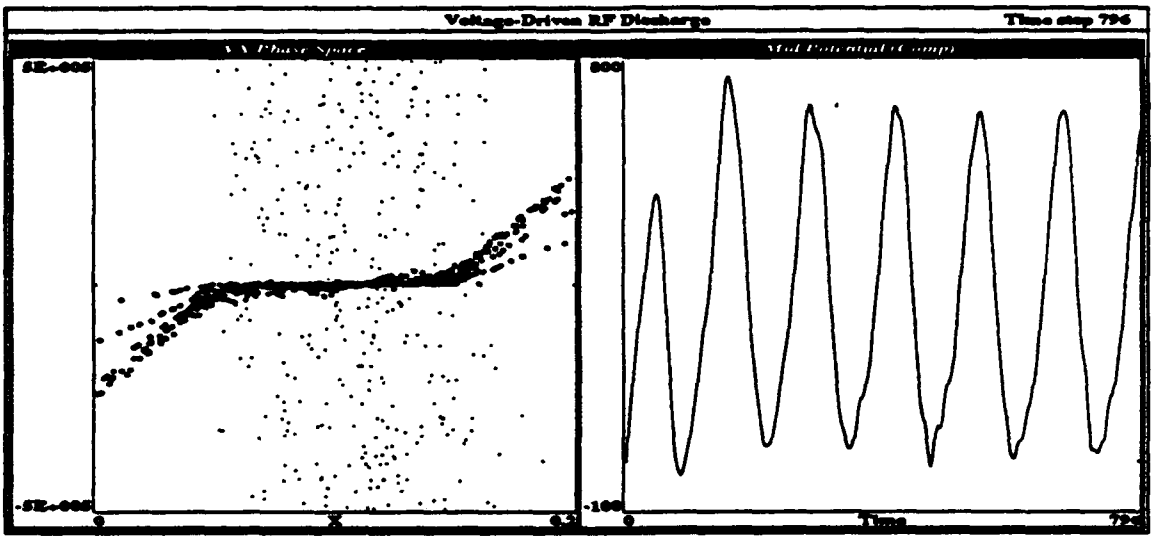

Figure 3. Enlarged to show ion velocities to the left; time response of mid-potential to the right.

ACKNOWLEDGMENTS

Work supported in part by DOE Contract DE-FG03-86ER53220 and ONR Contract N00014-85-K-0809.
Development was done on IBM PC-AT's under DACE grant and on IBM PS/2 Model 80 under IBM Courseware Program, for which we are most grateful.

---

[1] J. P. Verboncoeur and V. Vahedi to be presented at this conference (1989).

[2] L. R. Peterson and J. E. Allen, Jr. J. Chem. Phys., 56, 6068 (1972).

[3] E. A. Den Hartog, D. A. Doughty and J. E. Lawler, Phys. Rev. A, 38, 2471 (1988).

The Traveling-Wave-Tube Code IBC

by I.J. Morey and C.K. Birdsall
ERL, University of California, Berkeley, CA 94720

IBC (Interactive Beam-Circuit) is a one-dimensional many particle, traveling-wave-tube simulation code which has been developed to run interactively on a PC or Workstation. The code follows all of the particles in the tube, rather than just those in one wavelength. This allows for nonperiodic inputs, nonuniform line and a large set of spatial diagnostics which can be displayed graphically.

The code uses particle-in-cell techniques (Birdsall and Langdon, 1985) to model the motion of beam electrons and simple finite difference methods to model the fields of the coupled slow-wave transmission line. The coupling between the beam and the transmission line is based upon the finite difference equations of Brillouin (1949), and particle-in-cell techniques are also used to include the space-charge effects, in a manner similar to that used by Hess (1961).

The transmission line equations used in the code are:

$$\frac{V_i^t - V_i^{t-1}}{\Delta t} = -\frac{1}{C}\frac{I_{i+1/2}^{t-1/2} - I_{i-1/2}^{t-1/2}}{\Delta x} + \frac{\kappa(k)}{C}\frac{Q_{b,i}^t - Q_{b,i}^{t-1}}{\Delta t}, \tag{1}$$

$$\frac{I_{i-1/2}^{t+1/2} - I_{i-1/2}^{t-1/2}}{\Delta t} = -\frac{1}{L}\frac{V_i^t - V_{i-1}^t}{\Delta x}. \tag{2}$$

The variables V_i^t and $I_{i+1/2}^{t+1/2}$ are the transmission line voltage and current at the points $i\Delta x$ and $(i+1/2)\Delta x$ respectively, and at times $t\Delta t$ and $(t+1/2)\Delta t$ respectively. The capacitance and inductance per unit length are C and L. The beam charge within a section of the tube, $Q_{b,i}$, induces a charge on the transmission line $\kappa(k)Q_{b,i}$, where k is the wavenumber of the space-charge waves. The factor $\kappa(k)$ reflects the nature of the space-charge coupling constants for finite diameter TWT and depends on the relative diameters of the beam and the waveguide, and the transverse field profiles of the different wave modes.

From the equation of continuity, another driving term could be used, similar to Pierce (1950):

$$-\frac{\kappa(k)}{C}\frac{I_{b,i+1/2}^{t-1/2} - I_{b,i-1/2}^{t-1/2}}{\Delta x}. \tag{3}$$

This option is available in the code. Using a method of assigning the charge of each electron particle to the two nearest cell boundaries and the current of each electron particle to the two nearest cell centers, these two driving terms produce the same growth (satisfying continuity).

We assume that the space-charge field variables have a radial profile of the form $J_0(k_\perp r)$ (TM_{01} mode), where $k_\perp = 2.405/R_{beam}$ and R_{beam} is the beam radius. This implies that there is a conductor at the edge of the beam and allows Poisson's equation for the space-charge potential, ϕ, and density, ρ, in cylindrical coordinates to be simplified to

$$\frac{\partial^2 \phi}{\partial x^2} - k_\perp^2 \phi = -\frac{\rho}{\epsilon_0}, \tag{4}$$

where $\phi(x, r, \theta) = \phi(x) J_0(k_\perp r)$ and similarly for ρ. We also assume that there is no DC space charge because the unperturbed electron beam is neutralized by cold immobile ions. Therefore, even though the AC space-charge density has a $J_0(k_\perp r)$ profile, we can choose a uniform radial density profile for the beam and the ions.

An additional feature has also been added so that the effects of space charge can be observed easily. The constant *SCcoup* allows the user to change the strength of the space-charge force. When $SCcoup = 1$, the full effect of the space charge is included, but when $SCcoup = 0$ the space-charge force has no effect, so

$$E_{(total)i+1/2} = E_{(circuit)i+1/2} + SCcoup * E_{(space-charge)i+1/2}. \tag{5}$$

The same relationship applies to the total, circuit and space-charge potentials, and the electron bunching observed in IBC with $SCcoup = 1$ agrees with the results of Hess (1961).

The transmission line is terminated at both ends with a resistor and a voltage source. However, these terminations can be matched only when there is no beam-circuit coupling. The greater the coupling between the beam and the circuit, the greater the reflected signal. If the loop gain exceeds unity, the tube will become an oscillator. To avoid this, a section of the transmission line can be made lossy, or, an absorbing termination length may be added to the tube - a region where the loss increases exponentially and the beam-circuit coupling decays to zero.

The boundary conditions for the particles are absorption at both the source and collector. The beam particles are injected uniformly at the source. The space-charge potential is fixed at zero at both the source and collector.

When the code is run on an IBM PS2, with 100-200 cells and up to 5 particles per cell, many different features of a TWT interaction can be observed in a one hour session. Quantities such as: the beam density and current, the two driving terms, the circuit voltage and current and the power, can be displayed individually or all together. The following diagrams show the output for a tube of length 0.2 meters, a gain of $C = 0.056$ and an absorbing termination.

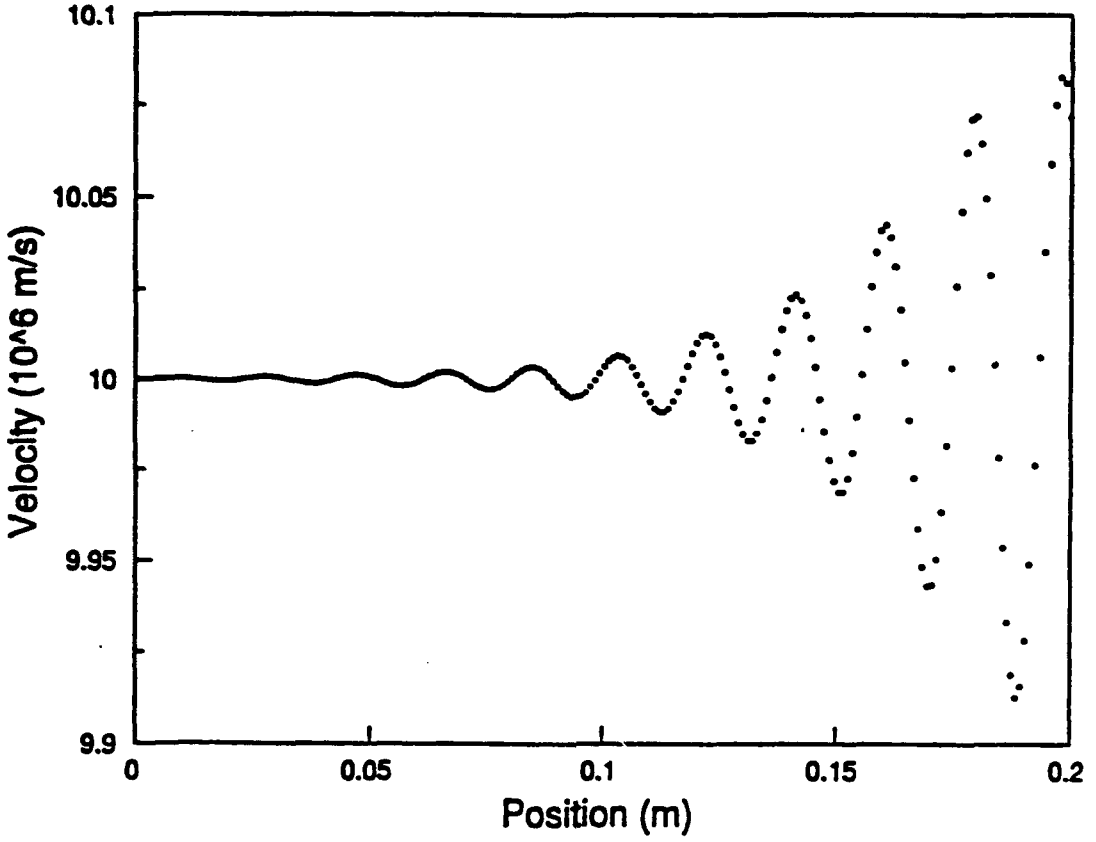
10.1
10.05
10
9.95
9.9
Velocity (10^6 m/s)
0
0.05
0.1
0.15
0.2
Position (m)

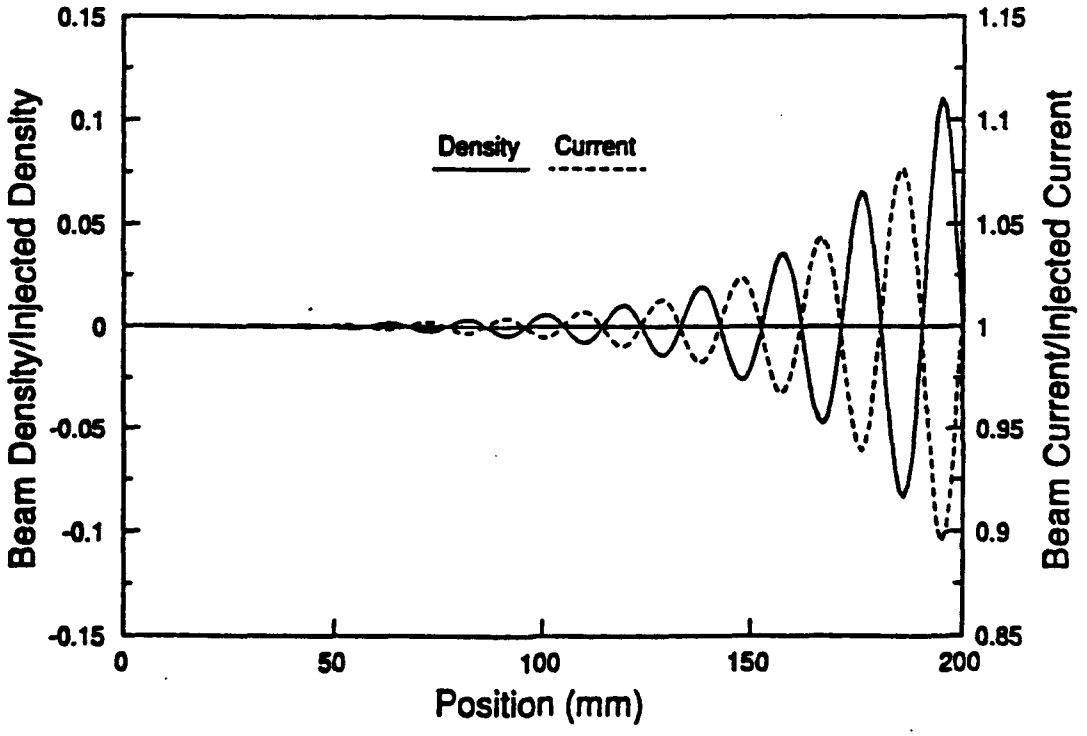
0.15
0.1
0.05
0
-0.05
-0.1
-0.15
Beam Density/Injected Density
Density
Current
1.15
1.1
1.05
1
0.95
0.9
0.85
Beam Current/Injected Current
0
50
100
150
200
Position (mm)

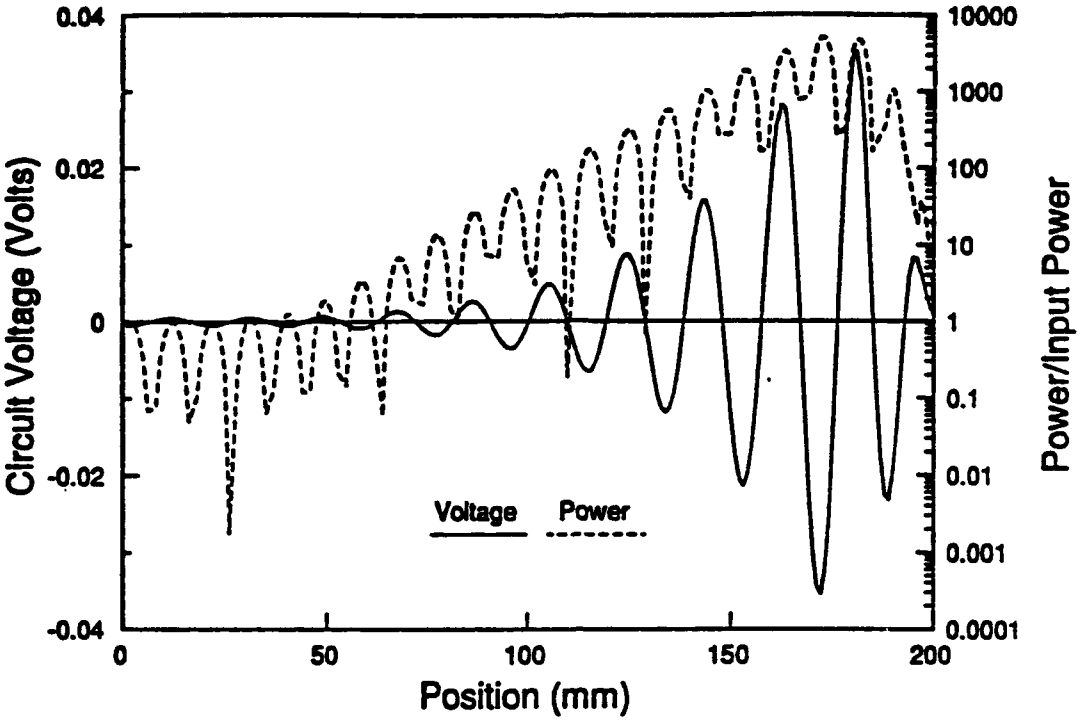

This work was supported by a sub-contract from Prof. N. Luhmann, UCLA, Air Force Contract F30602-87-0201, and by a gift from IBM.

References

C.K. Birdsall and A.B. Langdon, *Plasma Physics via Computer Simulation*, McGraw Hill, New York, 1985.

L. Brillouin, The Traveling-Wave Tube (Discussion of Waves for Large Amplitudes), J. App. Phys., 20, 1196-1206, 1949.

R.L. Hess, Large-Signal Traveling Wave Tube Operation: Concepts and Analysis, USAF Aeronautical Systems Division Technical Report 61-15, 1961.

J.R. Pierce, *Traveling Wave Tubes*, D. Van Nostrand, New York, 1950.

PDC1: ONE DIMENSIONAL RADIAL CODE FOR A CYLINDRICAL PLASMA DEVICE WITH AN EXTERNAL RLC CIRCUIT

M. Virginia Alves[1], Vahid Vahedi, Charles K. Birdsall
Plasma Theory and Simulation Group
Electronics Research Laboratory
University of California
Berkeley,CA 94720

PDC1 is a one dimensional (radial), electrostatic particle simulation code with the plasma bounded by two concentric cylinders. These electrodes can be coupled to an external circuit as shown in Figure 1. Only spatial variations in r are considered. The principles applied in this code are the same as those used in the planar model code PDW1, widely used since 1983 [1].

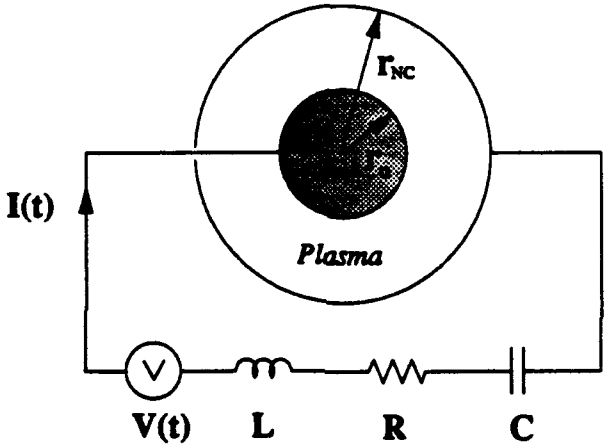

Figure 1. Cylindrical plasma device with an external RLC circuit.

PDC1 is very flexible and runs in the WinGraphics environment [2]. It is being applied, for example, to RF discharges, in which the RF powered electrode and the grounded electrode have different areas, and to Plasma Immersion Ion Implantation. For convenience, the inner cylinder is considered powered and the outer cylinder is grounded. In addition, in 1D-3V (r, v_r, v_θ, v_z) with an applied axial magnetic field, B_{z0}, many magnetized non-neutral plasma problems may be addressed, with or without the center cylinder.

We obtain the finite difference equations for fields (E) and potential (ϕ) related to density (ρ), on a spatial grid, using Gauss' law, in order to guarantee conservation of flux. The particles are considered to be cylindrical shells, uniform along z. The grid quantities are indexed by j. The grid points are spaced uniformly in r, $\Delta r \equiv \frac{r_{NC} - r_0}{NC}$, where NC is the number of cells, and r_0 and r_{NC} are the inner and outer cylinder radius. The charge weighting guarantees charge conservation.

---

1. Visiting from Institute for Space Research INPE, P.O. 515, 12201- S. J. Campos, SP, Brazil

Applied to the cylindrical surface at $j+\frac{1}{2}$, Gauss' law produces the radial electric field from the charges as in Birdsall and Langdon [3]:

$$\frac{Q_j}{\varepsilon} = 2\pi r_{j+\frac{1}{2}} E_{j+\frac{1}{2}} - 2\pi r_{j-\frac{1}{2}} E_{j-\frac{1}{2}} \qquad \text{where} \quad r_{j+\frac{1}{2}} \equiv \frac{r_{j+1}+r_j}{2} \quad \text{and} \quad j>0 \tag{1}$$

For $j = 0$ we have:

$$\frac{Q_0}{\varepsilon} = 2\pi r_{\frac{1}{2}} E_{\frac{1}{2}} - 2\pi r_0 E_0 \tag{2}$$

In order to obtain an equation in ϕ, we use single cell differencing:

$$E_{j+\frac{1}{2}} = -\frac{\phi_{j+1}-\phi_j}{\Delta r_{j+\frac{1}{2}}} \qquad \text{where} \quad \Delta r_{j+\frac{1}{2}} \equiv r_{j+\frac{1}{2}} - r_{j-\frac{1}{2}} \tag{3}$$

The charge density is obtained from $\rho_j = \frac{Q_j}{V_j}$, where $V_j \equiv \pi(\Delta r^2)_j$ with:

$$(\Delta r^2)_j = r^2_{j+\frac{1}{2}} - r^2_{j-\frac{1}{2}} \qquad j>0 \tag{4}$$

$$(\Delta r^2)_0 = r^2_{\frac{1}{2}} - r^2_0 \tag{5}$$

Using (3)-(5) in (1) and (2) we obtain a three-point finite difference form of Poisson's equation:

$$-r_j \Delta r^2 \frac{\rho_j}{\varepsilon} = (r_j - 0.5)\phi_{j-1} - 2r_j\phi_j + (r_j + 0.5)\phi_{j+1} \qquad j>0 \tag{6}$$

$$\phi_1 - \phi_0 = -\Delta r \frac{(r_0 + 0.25)\Delta r \frac{\rho_0}{2} + r_0\sigma}{(r_0 + 0.5)\varepsilon} \tag{7}$$

In (6) r_j were normalized by Δr, and to derive (7), we assume $E_0 = \frac{\sigma}{\varepsilon}$, where σ is the charge surface density at the inner cylinder. Equation (7) is one of the boundary conditions used to solve the Poisson equation. The second boundary condition is obtained assuming that the outer electrode is at the reference potential, $\phi_{NC} = 0$.

Equations (6)-(7) provide a tridiagonal matrix which is solved to find the potentials ϕ_j. Then the electric fields are obtained using:

$$E_j = -\frac{\phi_{j+1}-\phi_{j-1}}{2\Delta r} \qquad \text{for} \quad j = 1,2,\ldots,NC-1$$

The electric field at the first grid point is obtained from (2); for the last grid point we use a similar equation for E_{NC}.

In order to solve equations (6)-(7) for the potentials, the charge density must be known on the same grid. The weighting used to accumulate charge is similar to linear weighting. We use the area of rings to weight the charges ([3]; without variations in θ).

The weighting of the electric field to the particles is done in the same manner. The charge accumulated on the grid point at the boundary is some fraction (in PDW1, exactly $\frac{1}{2}$, [1]) of that which would be accumulated at the grid point which is not at a boundary if the physical charge density were the same at the two points. To compensate for this we use a volume corresponding to half a cell (see eq.(5)) when we define charge density at the last grid points ($j=0$, $j=NC$).

In order to load the system at $t=0$ with a uniform density, we assume a constant density in r equal to $\frac{N}{\pi(r_{NC}^2 - r_0^2)\Delta r^2}$ where N is the total number of particles to load the system. Since the density is uniform in r, at each position r_i we have:

$$r_i^2 - r_{i-1}^2 = \frac{r_{NC}^2 - r_0^2}{N} \qquad (8),$$

where r_{i-1} is the position of the previous particle. The algorithm (8) is used to determine the positions of the particles at $t=0$.

The cylindrical plasma device with an external circuit RLC is showed in Figure 1. In order to solve the circuit equation we use the 2nd order backward Euler method and we treat four different cases (as in PDW1 [4]):

a) C=0, open circuit;
b) current source;
c) R = L = 0 and $C \rightarrow \infty$, short circuit;
d) general case: RLC circuit with voltage source.

It is important to consider carefully the relation between σ and ϕ_0 in order to specify the correct boundary condition for solving Poisson's equation.

Cylindrical computer experiments were performed many years ago with 1D models in order to ascertain the possibility of electrostatic inertial confinement [5] and the dynamics of limiting charge and current [6].

The following plots illustrate a run of PDC1 for an RF discharge driven by a current source displaying the velocity phase space (velocity versus position for each particle), the potential across the bounded region as a function of position, and the time history of the potential at the inner electrode.

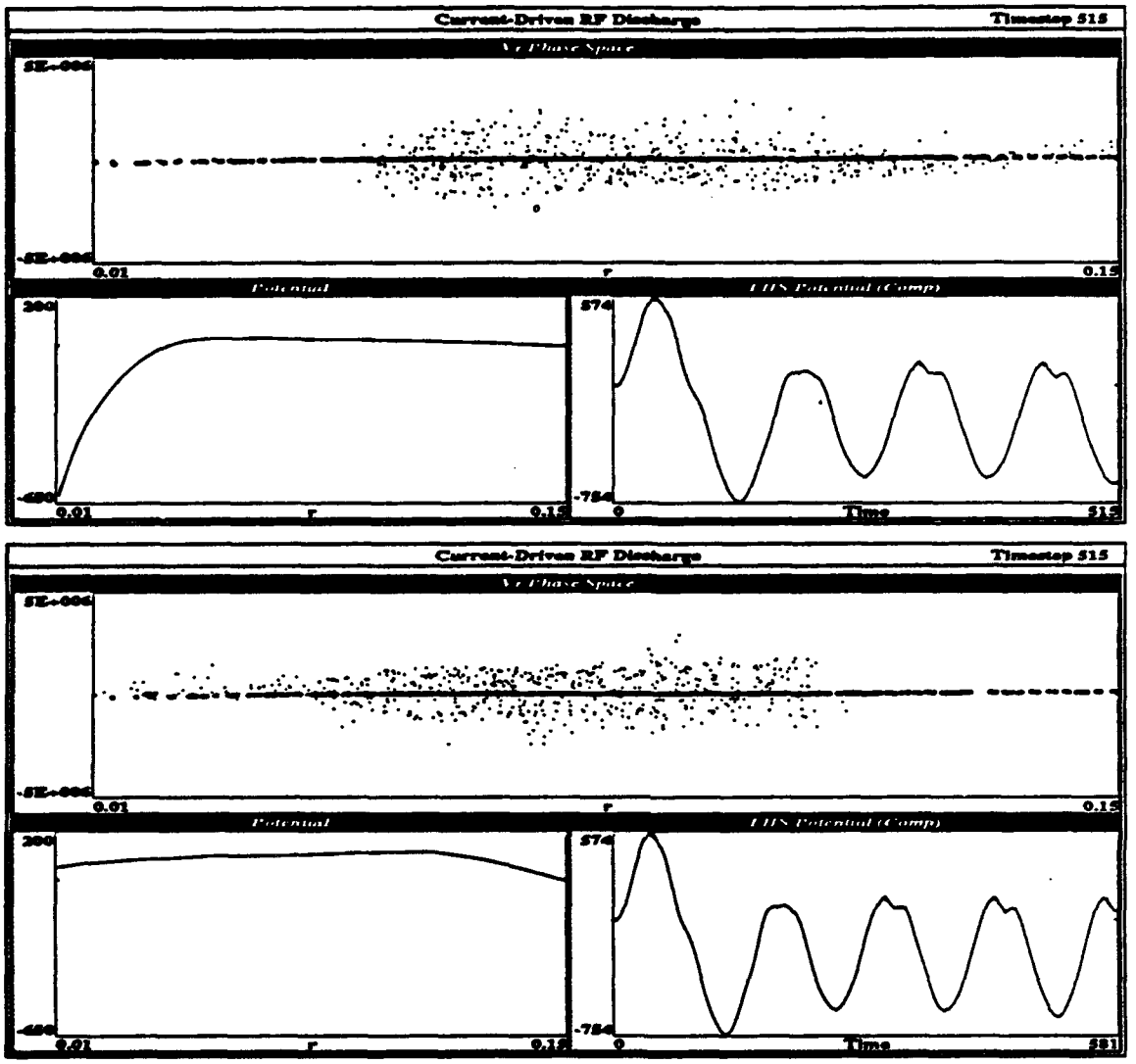

ACKNOWLEDGEMENTS

Work supported in part by DOE Contract DE-FG03-86ER53220 and ONR Contract N00014-85-K-0809.
M. V. Alves supported partially by *CAPES-Ministry of Education, Brazil.*
Development was done on IBM PC-AT's under DACE grant and on IBM PS/2 model 80 under *IBM Courseware Program*, for which we are most grateful.

---

[1] W. L. Lawson, *J. Comp. Phys.* 80, 253 (1989).

[2] J. P. Verboncoeur and V. Vahedi to be presented at this conference (1989).

[3] C. K. Birdsall and A. B. Langdon, *Plasma Physics via Computer Simulation*, McGraw-Hill (1985).

[4] I. J. Morey, J. P. Verboncoeur, V. Vahedi, to be presented in this conference (1989).

[5] C. W. Barnes, *The Computer Simulation of a Spherically Symmetric Plasma*, SUIPR Report No.344, Stanford University (1970).

[6] R. W. Hockney, *J. Appl. Phys.* 39, 4166 (1968).

Multi-Scale Particle Simulation of Bounded Plasmas

S. E. Parker*, A. Friedman**, S.L. Ray** and C. K. Birdsall*

*Electronics Research Laboratory, University of California, Berkeley CA 94720

**Lawrence Livermore National Laboratory, Univ. of California, Livermore CA 94550

1 Introduction

We are using the multi-scale technique [1] to model bounded systems. Certain bounded systems are a naturally suited for the multi-scale method because the boundary layer (or sheath) that forms at the wall, which is usually a short spatial ($\sim \lambda_{De}$) and time scale ($\sim \omega_{pe}$) structure, can significantly affect the bulk plasma behavior. One goal is to understand the interaction between the bulk plasma and the sheath. If the relevant short time scale physics is local to a few (or one) known spatial regions, then one can take advantage of this by advancing particles with variable Δt depending on position, hence reducing computing time. The unmagnetized sheath problem is such a case.

The model is a one dimensional bounded slab with kinetic ions and electrons. We start with a collisionless and unmagnetized system for simplicity. The right boundary is a conducting wall that absorbs all particles that come in contact with it. The left boundary is a symmetry point, where the particles are reflected. We allow a specified initial distribution: $f(x, v, t = 0)$.

In order to test the numerics of both the multi-scale method and boundary conditions we are using the following test problem: a cutoff Maxwellian distribution for the electrons and fixed (or infinitely massive) ions. The system has an analytic solution, so the run may be started from equilibrium. This gives us a benchmark and tests the fast time scale electron sheath dynamics. Results using variable Δt (with ratio of smallest to largest of 1:128) will be given. In the future, we intend to use the more general model to study time dependent bounded plasma problems, such as a plasma expanding toward a conducting wall.

2 The Multi-Scale Method

The goal is to model bulk, macroscopic ($\omega \ll \omega_p$, $\lambda \gg \lambda_D$) plasma phenomena globally, *while also* accurately treating short time ($\sim \omega_p^{-1}$) and short space scales ($\sim \lambda_D$) in *local* regions where microscopic physics is important (e.g. sheaths). We accomplish this by allowing groups

of particles to move at different Δt's. The Direct Implicit method is used to allow for large $\omega_p \Delta t$ [2]. Each group of particles (call them G_m), is pushed every 2^m time steps, using $\Delta t_m = 2^m \delta t$, $m = 0, 1, 2, ...$, where δt is the smallest time increment. In order to avoid having "special" time steps, we do not move all the particles of a given group at once. We define subgroups of G_m called blocks (call them B_m^l). Given a group G_m, there are 2^m blocks B_m^l, where $l = 0, 1, 2, ..., (2^m - 1)$. Each block in a group is moved at a different time step. We move a block B_m^l at time step n, with $t = n\delta t$, when: $(n) mod (2^m) = l$. As an example, consider 3 groups ($m = 0, 1, 2$):

Group	Step size	Block	When pushed
G_0	$\Delta t_0 = \delta t$	B_0^0	every step
G_1	$\Delta t_1 = 2\delta t$	B_1^0	even steps
		B_1^1	odd steps
G_2	$\Delta t_2 = 4\delta t$	B_2^0	if n mod 4 = 0
		B_2^1	if n mod 4 = 1
		B_2^2	if n mod 4 = 2
		B_2^3	if n mod 4 = 3

To illustrate how particles are moved, take time step n=7:

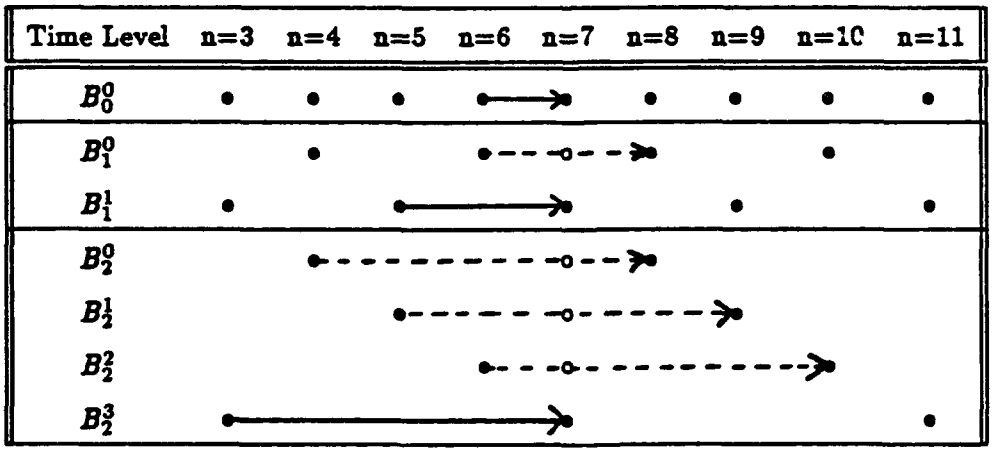

Three blocks are moved at n=7: B_0^0, B_1^1 and B_2^3 (represented by the solid arrows). Contributions to the free streamed charge density $\tilde{\rho}$, and the "effective" susceptibility χ from all blocks are known in advance of the step; those from blocks B_1^0, B_2^0, B_2^1 and B_2^2, have been obtained by interpolation in time. Thus, the field is known before the blocks: B_0^0, B_1^1 and B_2^3 are advanced to n=7.

3 Physics of the Test Problem

The sheath problem we use is a simple example to test the electron sheath dynamics. $f(x,v)$ for the electrons is a cut-off Maxwellian:

$$f(x,v) = \begin{cases} n_0 c_0 \exp\left(-\frac{\frac{1}{2}mv^2}{T} + \frac{e\phi(x)}{T}\right); & |v| < v_c(x), \\ 0; & |v| \geq v_c(x). \end{cases} \tag{1}$$

where $n_0 = n_e(x=0)$, $mv_T^2 = T$, $c_0 = \left\{2\sqrt{2}\, v_T \operatorname{erf}\left(\frac{\sqrt{2}}{2}\frac{v_0}{v_T}\right)\right\}^{-1}$ and, $v_0 = v_c(x=0)$. The ions are fixed: $n_i(x) = n_0$ Changing variables; $u = \frac{\sqrt{2}}{2}\frac{v}{v_T}$, and $\psi = \frac{e\phi}{T}$, Poisson's equation becomes:

$$\frac{d^2\psi}{dx^2} = \frac{1}{\lambda_D^2}\left\{\frac{e^{\psi}\operatorname{erf}\sqrt{u_0+\psi}}{\operatorname{erf}\sqrt{u_0}} - 1\right\} \tag{2}$$

We can now solve Eq. (2) with the appropriate boundary conditions, and knowing $\phi(x)$ we load the particles (electrons) according to Eq. (1).

4 Comparison of Computing Time

Comparison of cpu time for two runs: one with 1 Δt group and the other with 8 Δt groups. No. of particles = 100,000; no. of timesteps = 10,000. Time is given in microseconds per particle per timestep.

$\frac{\text{largest } \Delta t}{\text{smallest } \Delta t}$:	1	128	Gain
total time :	4.62	1.56	2.96
without io :	3.75	0.670	5.60
without io, or initialization. :	3.63	0.546	6.64

We have not yet fully vectorized the code. There is still room for optimization, although the logic involved in changing particles from block to block makes vectorization more complicated.

Acknowledgements

This work is supported by DOE contract DE-FG03-86ER53220 and ONR contract N00014-85-K-0809.

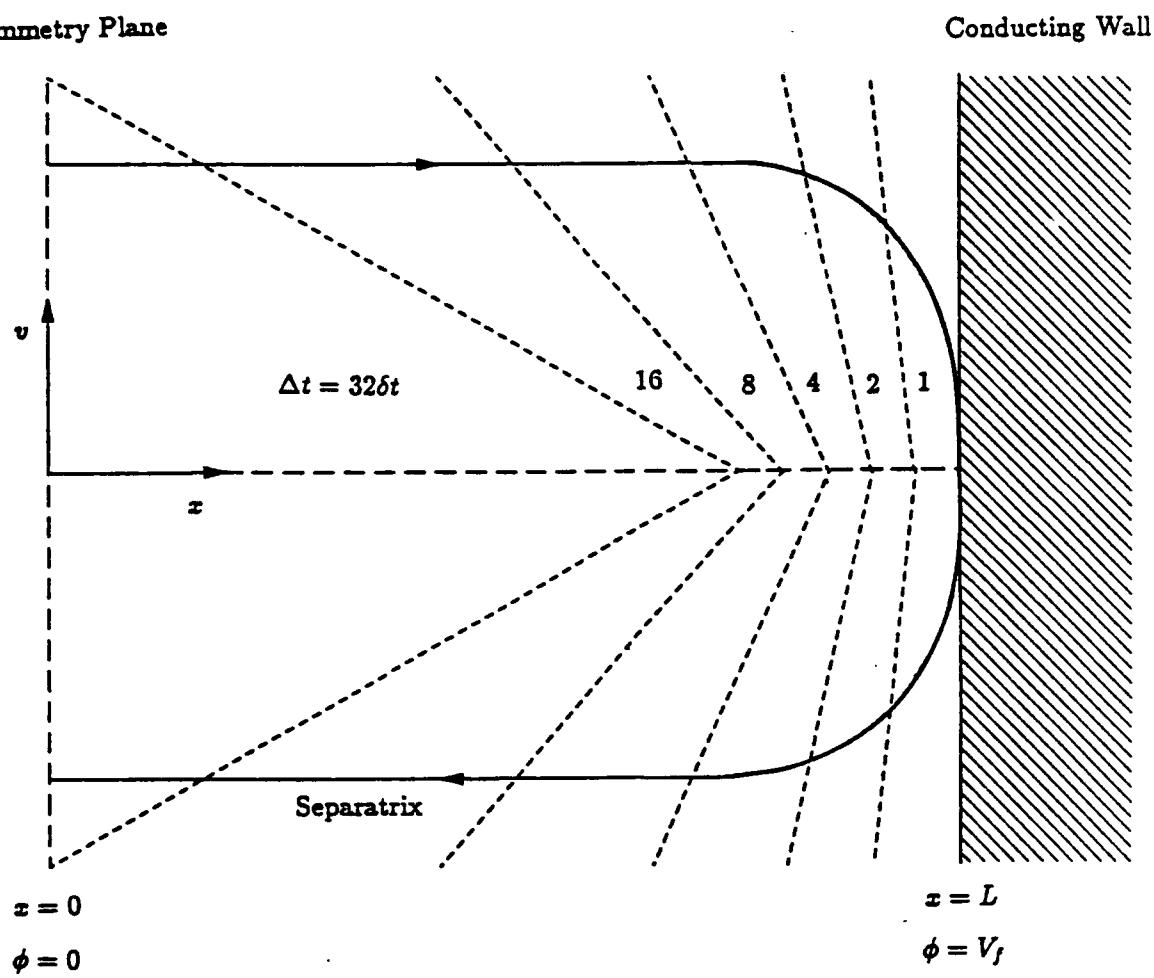

Figure 1: Schematic of phase space for the bounded multiscale simulation. The case shown has 6 groups. Particles change Δt groups as they move in phase space. The solid line represents the separatrix, $v_c(x)$, where inside the particles are trapped and outside the particles hit the wall and are absorbed. The ion are fixed and the electrons have a cut-off Maxwellian distribution. The conducting wall is left floating, V_f.

References

[1] "Particle-In-Cell Plasma Simulation with a Wide Range of Space and Time Scales ", A. Friedman, S.L. Ray, C.K. Birdsall and S.E. Parker, Proc. 12th Conf. on Numerical Simulation of Plasmas, APS, San Francisco, CA, Sept. 1987.

[2] "Direct Implicit Particle Simulation", A.B. Langdon, D.C. Barnes, from *Multiple time scales*, J.U. Brackhill and B.I. Cohen, editors, Academic Press, 1985.

A Particle-In-Cell Method for Modeling Small Angle Coulomb Collisions in Plasmas

S. E. Parker

Electronics Research Laboratory, University of California, Berkeley CA 94720

1 Introduction

We propose a computational method to self-consistently model small angle collisional effects. This method may be added to standard Particle-In-Cell (PIC) plasma simulations to include collisions, or as an alternative to solving the Fokker-Planck (FP) equation using finite difference methods. The distribution function is represented by a large number of particles. The particle velocities change due to the drag force, and the diffusion in velocity is represented by a random process. This is similar to previous Monte-Carlo methods [1,2], except we calculate the drag force and diffusion tensor self-consistently. The particles are weighted to a grid in velocity space and the associated "Poisson equations" are solved for the Rosenbluth potentials. The motivation is to avoid the very time consuming method of Coulomb scattering pair by pair. First the approximation for small angle Coulomb collisions is discussed. Next, the FP-PIC collision method is outlined. Then we show a test of the particle advance modeling an electron beam scattering off a fixed ion background.

2 Small angle Coulomb collisions

The FP equation for describing small angle Coulomb collisions can be solved numerically using finite difference techniques. An alternate method is to follow the evolution of a large number of particles. Using the notation of Trubnikov [3], an infinitestimal "cloud" of test particles can be represented by the quantities $< \Delta v_i >$ and $< \Delta v_i \Delta v_j >$ to the same order of accuracy as the FP equation[4], and are defined by:

$$< \Delta v_i > \equiv \frac{d\bar{v}_i(t)}{dt} \tag{1}$$

$$< \Delta v_i \Delta v_j > \equiv \frac{d}{dt}\left\{\overline{(v_i - \bar{v}_i)(v_j - \bar{v}_j)}\right\} \tag{2}$$

The bars represent averages. These may be interpreted as ensemble averages over many initial states, or as an ordinary average by letting the number of particles in a cloud, N, become large. We follow the second interpretation allowing a simpler simulation method.

$\bar{v}_i$ is now the average velocity of the local cloud. The i and j subscripts are the 3 velocity components in Cartesian coordinates, $(v_1 = v_x, v_2 = v_y, v_3 = v_z)$. $< \Delta v_i >$ is the drag force felt by an average particle in the cloud. $< \Delta v_i \Delta v_j >$ is the spreading or diffusion in velocity space of the cloud.

Numerically we advance the velocity of the particles by using the following equation [4]:

$$\Delta v_i(t^n) =< \Delta v_i > \Delta t + B_{ij}\Delta W_i(t^n) \tag{3}$$

where B_{ij} satisfies,

$$B_{ik}B_{kj} =< \Delta v_i \Delta v_j > \tag{4}$$

where $\Delta W_i(t^n) \equiv W_i(t^n) - W_i(t^{n-1})$, and $W_i(t)$ is a vector function that represents a Wiener process (or Brownian motion) having the following properties $< W_i(t) >= 0$ and $< W_i(t)W_j(t) >= t\delta_{ij}$. B and W are not unique and only need to satisfy the above criteria. In our model we choose:

$$\Delta W_i(t^n) = \sqrt{\Delta t} R_i \tag{5}$$

where R_i are independent random numbers satisfying $< R_i >= 0$, and $< R_i R_j >= \delta_{ij}$. We have found a a matrix B such that $BB^T = A$, given by:

$$B_{ij} = \begin{pmatrix} \sqrt{A_{11}} & 0 & 0 \\ \frac{A_{12}}{\sqrt{A_{11}}} & \sqrt{A_{22} - \frac{A_{12}^2}{A_{11}}} & 0 \\ \frac{A_{13}}{\sqrt{A_{11}}} & \frac{A_{23}}{B_{22}} - \frac{A_{12}A_{13}}{A_{11}B_{22}} & \sqrt{A_{33} - \frac{A_{13}^2}{A_{11}} - B_{32}^2} \end{pmatrix} \tag{6}$$

By letting $A_{ij} =< \Delta v_i \Delta v_j >$, we note that Eq. (6) satisfies Eq. (4) and can therefore use this B in Eq. (3).

The "field" quantities are obtained from two functions ϕ and ψ, the Rosenbluth potentials, which in turn are solved by the two Poisson equations [3]:

$$\nabla^2 \phi^\beta = f^\beta(v_i) \tag{7}$$

$$\nabla^2 \psi^\beta = \phi^\beta(v_i) \tag{8}$$

where β is the superscript representing the field species, $\beta = (i, e)$. Then $< \Delta v_i >$ and $< \Delta v_i \Delta v_j >$ are obtained in terms of the Rosenbluth potentials using the following equation (see reference [3] for a derivation):

$$< \Delta v_i >^\alpha = -\sum_\beta \left(1 + \frac{m_\alpha}{m_\beta}\right) L^{\alpha/\beta} \frac{\partial \phi_\beta}{\partial v_i} \tag{9}$$

$$< \Delta v_i \Delta v_j >^{\alpha} = -2 \sum_{\beta} L^{\alpha/\beta} \frac{\partial^2 \psi_\beta}{\partial v_i \partial v_j} \tag{10}$$

$L^{\alpha/\beta} = \lambda \left(\frac{4\pi e_\alpha e_\beta}{m_\alpha} \right)^2$ is a constant (given here in cgs units), and λ is the Coulomb logarithm. α and β represent the test and field particles, respectively (e.g. $\alpha = (i, e)$ and $\beta = (i, e)$).

3 Outline of the Method

For the particle advance, we start with the simplest scheme [1], similar to Euler's method, except there is an added diffusion term (the last term on the right):

$$v_i^{n+1} = v_i^n + < \Delta v_i >^n \Delta t + B_{ij}^n \sqrt{\Delta t} R_j \tag{11}$$

R_j are independent random numbers having the two properties given above. Following a methodology similar to PIC simulation, we weight the particles to a grid, calculate the field quantities, advance the particles and repeat the process. The basic algorithm is as follows:

Step 1. Weight the particles to a grid in velocity space using linear interpolation.

Step 2. Solve Eqs. (7) and (8) on the grid for ϕ and ψ.

Step 3. Obtain $< \Delta v_i >^n$ and B_{ij}^n on the grid using Eqs. (6), (9) and (10).

Step 4. For each particle, obtain $< \Delta v_i >^n$ and B_{ij}^n by interpolating from the grid to the particle location v_i. Then, update the velocity using Eq. (11).

4 Test of the particle advance

As an initial test of the particle advance, Eq. (11), we model an electron beam scattered by infinitely massive cold ions. For this test case $< \Delta v_i >$ and $< \Delta v_i \Delta v_j >$ are given by the two simple analytic expressions:

$$< \Delta v_i > = -C \frac{v_i}{v^3} \tag{12}$$

$$< \Delta v_i \Delta v_j > = C \left(\frac{\delta_{ij}}{v} - \frac{v_i v_j}{v^3} \right) \tag{13}$$

where $C = \frac{n_\beta L^{\alpha/\beta}}{4\pi}$. We do not calculate the field quantities on the grid (step 1 and 2 above), but rather, use Eqs. (12) and (13) directly. This provides a good test of the particle advance, Eq. (11). We expect the total x-momentum to be given by [3]:

$$p_{x,total}(t) = p_{x,total}(t = 0) exp \left(\frac{-C}{v_0^3} t \right) \tag{14}$$

where v_0 is the initial beam velocity. We have made a test run with the following parameters: $C = 1$, $v_0 = 1$, $v_{Te} = 0.01$ and $\Delta t = 0.001$. The energy error is less than 0.2 percent and the momentum error is less then 1 percent for a total time: T=1.

5 Future Work

We are developing a code to test the FP-PIC method outlined above. In the near future we plan to implement the algorithm in a 1d 3v electrostatic code in order to study combined collective electrostatic and collisional effects. With this code we would assume spatial homogeneity for calculating the collisional terms. If this assumption is not valid one would have to partition $f(v)$ into spatial regions j, and calculate $f_j(v)$ for each spatial region. One would have to ensure that enough particles in each spatial zone to adequately fill out the distribution function.

In addition, we need to address the accuracy and stability issues associated with this method, and study the feasibility of using a more accurate particle advancing scheme than that given by Eq. (11).

Acknowledgements

This work is supported by DOE contract DE-FG03-86ER53220 and ONR contract N00014-85-K-0809.

References

[1] "Transition from Pastukhov to Collisional Confinement in a Magnetic and Electrostatic Well", T. D. Rognlien and T. A. Cutler, Nuclear Fusion, **20** (1980) 8 1003.

[2] " Electron Energy Flow in a Collisional Scrape-off Plasma", R. Chordura, 12th Euro. Conf. on Plasma Phys., Budapest, Hungary, Sept. 1985.

[3] "Particle Interactions in a Fully Ionized Plasma", B. A. Trubnikov, p.105-204, *Reviews of Plasma Physics*, M. A. Leontovich ed., Consultants Bureau, New York, 1965.

[4] *Handbook of Stochastic Methods*, C. W. Gardiner, Springer-Verlag, New York 1985.

Comparison of Particle-In-Cell and Fokker-Planck Methods as Applied to the Modeling of Auxiliary-Heated Mirror Plasmas

Richard J. Procassini and Charles K. Birdsall
Electronics Research Laboratory
University of California, Berkeley, CA 94720

Bruce I. Cohen and Yoshi Matsuda
Lawrence Livermore National Laboratory
Livermore, CA 94550

1 Introduction

The transport and confinement of charged particles in an auxiliary-heated mirror plasma is modeled via the bounce-averaged Fokker-Planck (F-P) code SMOKE [2] and the direct-implicit particle-in-cell (PIC) code TESS [1]. The test case studied is that of a tandem mirror end plug which is heated by the injection of ECRH at both the fundamental and second harmonic of the electron gyrofrequency ($\omega_{RF,1} = \omega_{ce}$ and $\omega_{RF,2} = 2\omega_{ce}$). Figure 1 shows the magnetic field and potential profiles that are prescribed for the test case. Both electron-electron and electron-ion collisions are included. Each code employs a relativistic description of the electron dynamics in one spatial dimension. Each code follows the system to equilibrium, where the loss of particles (resulting from collisional detrapping of the loss-cone distribution) balances the trapping of particles (resulting from the preferential increase in the magnetic moment of the particle due to the resonant absorption of RF wave energy).

The modeling comparison is divided into three sections. The first entails benchmarking the

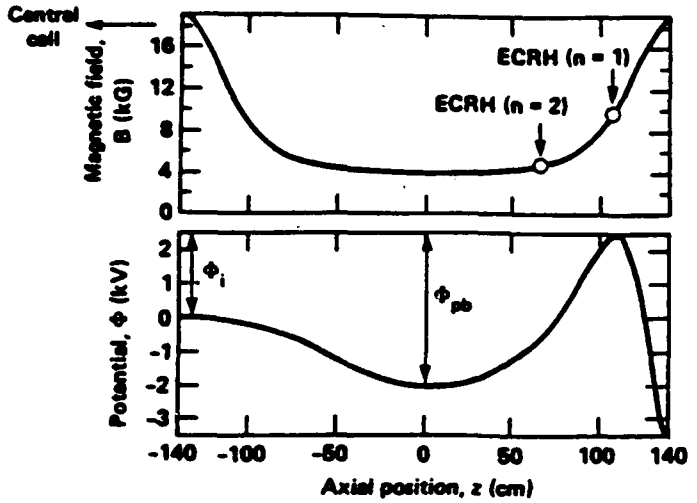

Figure 1: Magnetic field and potential profiles in the end plug of a tandem mirror plasma. The central cell is to the left, and the end wall is to the right.

physics results from the PIC code against those from the F-P code. The test case determines the confinement and transport of electrons *only*. The magnetic and electrostatic fields are prescribed quantities. Comparison is made of the electron velocity-space density contours at different axial locations, as well as the electron density and kinetic energy profiles. In order to determine the effect of particle counting statistics on these quantities, the PIC code is run with varying numbers of simulation electrons. The PIC code is also run including the ions, and a self-consistent calculation of the electrostatic potential. This last run allows us to determine the accuracy of the assumed potential profile used in the other runs. Next, a computational cost analysis is performed on each code. In addition to comparing the total run time for each of the codes, various code dependent costs are provided, such as the cost to push a particle each time step in the PIC code and the cost to "invert" the phase-space matrices in the F-P code. Finally, the advantages and disadvantages of each code are discussed in the context of the chosen test case, including a comparison of the effort involved in setting up the input deck for each code.

2 The Multiregion Bounce-Averaged Fokker-Planck Code

The SMOKE code determines the evolution of a particle distribution function f resulting from Coulomb collisional and RF-induced velocity space diffusion. The code numerically solves the

relativistic Fokker-Planck kinetic equation

$$\frac{\partial f}{\partial t} + \mathbf{v} \cdot \frac{\partial f}{\partial \mathbf{x}} + \frac{\partial}{\partial \mathbf{p}} \cdot \left[q \left(\mathbf{E} + \frac{1}{c} \mathbf{v} \times \mathbf{B} \right) f + \Gamma_{coll} + \Gamma_{rf} \right] = 0, \tag{1}$$

where t is the time, $\mathbf{x}$ is the position, $\mathbf{v}$ is the velocity, $\mathbf{p} \equiv \gamma m \mathbf{v}$ is the momentum, $\gamma \equiv (1 - v^2/c^2)^{-1/2}$ is the relativistic factor, m is the rest mass, c is the speed of light, $\mathbf{E}$ and $\mathbf{B}$ are of the electric and magnetic fields (static and RF components), and Γ_{coll} and Γ_{rf} are the fluxes arising from Coulomb collisional and RF wave interactions respectively. Since the bounce time of particles in the mirror (τ_b) is much smaller than the collisional or RF diffusion times (τ_{coll}, τ_{rf}), a bounce-averaged version of the F-P equation [3] is solved in (ε, μ) phase space

$$\tau_b \frac{\partial f}{\partial t} = \frac{\partial}{\partial \varepsilon} \left(D_{\varepsilon\varepsilon} \frac{\partial f}{\partial \varepsilon} + D_{\varepsilon\mu} \frac{\partial f}{\partial \mu} + D_\varepsilon f \right) + \frac{\partial}{\partial \mu} \left(D_{\mu\varepsilon} \frac{\partial f}{\partial \varepsilon} + D_{\mu\mu} \frac{\partial f}{\partial \mu} + D_\mu f \right), \tag{2}$$

where $\varepsilon \equiv (\gamma - 1)mc^2 + q\Phi$ is the total energy, $\mu \equiv p_\perp^2 / 2mB_0$ is the magnetic moment and $\tau_b \equiv \oint dz / |v_\parallel|$ is the particle bounce time. Each of the coefficient $D_{\alpha\beta}$ have contributions from Coulomb collisional and RF wave interactions. The quasilinear model of Bernstein and Baxter [3] is used to model the RF-induced diffusion.

The bounce-averaged F-P equation (2) is solved for the various regions (trapped-particle populations) via a two-step process. First, the (ε, μ) phase space is mapped into a rectangular (Cartesian coordinate) region (x, y). Second, a Galerkin finite-element method is used to solve (2) in the (x, y) phase space. (The same procedure is used to solve Poisson's equation for the Rosenbluth potentials.)

3 The Direct-Implicit Particle-In-Cell Code

The TESS code computes the trajectories of individual charged particles in either a prescribed or self-consistent electrostatic potential, and a prescribed magnetic field. The implicit nature of the code allows one to simulate long-wavelength, low-frequency phenomena, without having to resolve high-frequency effects, such as electron plasma oscillations. A relativistic guiding center formulation of the equations of motion in one spatial dimension ($\hat{z}$) is used

$$\begin{aligned} \frac{dz}{dt} &= \frac{p_z}{\gamma m} \\ \frac{dp_z}{dt} &= qE_z - \frac{\mu}{\gamma} \nabla B_z + \left(\frac{dp_z}{dt} \right)_{coll} + \left(\frac{dp_z}{dt} \right)_{rf} \\ \frac{d\mu}{dt} &= \left(\frac{d\mu}{dt} \right)_{coll} + \left(\frac{d\mu}{dt} \right)_{rf}. \end{aligned} \tag{3}$$

In general, the code simulates the transport and confinement of both ions and electrons. The self-consistent ambipolar potential is then calculated via the direct-implicit form of Poisson's equation

$$-\nabla \cdot \left(1 + \sum_s \chi_s\right) \nabla \Phi(z) = 4\pi e \left(Z n_i(z) - n_e(z)\right), \tag{4}$$

where the summation is over species s (ions and electrons), n_s is the free-streaming or explicit density of species s and χ_s is the implicit susceptibility which accounts for the implicit correction to the free-streaming density. The equations of motion (3) and modified Poisson equation (4) are solved via standard finite difference techniques. A self-consistent, relativistic, Monte Carlo binary collision model [4] and a quasilinear RF diffusion model [5] (after Bernstein and Baxter [3], as implemented by Rognlien [6]) are also included.

Acknowledgments

This research was sponsored by the Plasma Physics Research Institute under the auspices of the U. S. Department of Energy at the Lawrence Livermore National Laboratory under Contract Number W-7405-Eng-48.

References

[1] B. I. Cohen, J. C. Cummings, R. J. Procassini and C. K. Birdsall, "Direct Implicit Particle Simulation of Mirror Transport", *12th Conf. Num. Sim. of Plasmas*, Paper PW15, San Francisco, CA (1987).

[2] Y. Matsuda and J. J. Stewart, *J. Comput. Phys.*, 66, 197 (1986).

[3] I. B. Bernstein and D. C. Baxter, *Phys. Fluids*, 24, 108 (1981).

[4] R. J. Procassini, C. K. Birdsall, E. C. Morse and B. I. Cohen, "A Relativistic Monte Carlo Binary Collision Model for use in Plasma Particle Simulation Codes", Electronic Research Laboratory Memo UCB/ERL M87/24, University of California, Berkeley (1987).

[5] R. J. Procassini and B. I. Cohen, "Auxiliary Plasma Heating and Fueling Models for use in Particle Simulation Codes", Lawrence Livermore National Laboratory Report UCID-21654 (1989).

[6] T. D. Rognlien, *Phys. Fluids*, 26, 1545 (1983).

DISTRIBUTION LIST

AFWL/DYP
Pettus

Department of Energy
Crandall, Katz, Lankford, Macrusky, Manley, Sadowski, Tech. Info. Center

Department of Navy
Condell, Florance, Roberson

Argonne National Laboratory
Brooks

Air Force Weapons Laboratory
Godfrey

Austin Research Associates
Drummond, Moore

Bell Telephone Laboratories
Hasegawa

Berkeley Research Assoc.
Brecht, Orens

Cal. Inst. of Technology
Bridges, Gould

Calif. State Polytech. Univ.
Rathmann

Cambridge Research Labs.
Rubin

Columbia University
Chu

Cornell University
Otani

Dartmouth
Hudson, Lotko

E. P. R. I.
Scott

GA Technologies
Bernard, Evans, Helton, Lee

Goddard Space Flight Center
Storey

GTE Laboratories
Rogoff, Winsor

Hascomb Air Force Base
Rubin

Hewlett-Packard Laboratories
Gleason, Marcoux

Hughes Aircraft Co., Torrance
Adler, Longo

Hughes Research Lab., Malibu
Harvey, Hyman, Poeschel, Schumacker

Institute of Fusion Studies, Texas
Librarian

JAYCOR
Klein, Tumolillo

JPL
Liewer

Kaman Science Corp.
Hobbs

Lawrence Berkeley Laboratory
Cooper, Kaufman, Kunkel,

Lawrence Livermore National Lab.
Albritton, Anderson, Brengle, Briggs, Byers, Chambers, Chen, B.Cohen, R. Cohen, Denavit, Estabrook, Fawley, Friedman, Fuss, Harte, Hewett, Kruer, Langdon, Lasinski, Lee, Matsuda, Max, Nevins, Nielsen, Smith, Tull, Ziolkowski

Lockheed
Siambis

Los Alamos Scientific Lab.
Barnes, Borovsky, Forslund, Kwan, Lindemuth, Mason, Nielson, Oliphant, Peratt, Sgro, Thode

M2 Microtek
Phillips, Snyder

Mass. Inst. of Technology
Bers, Lane, Palevsky

Mission Research Corporation
Mostrom

Nasa - Lewis Research Center
Freeman

Naval Research Laboratory
Armstrong, Boris, Craig, Haber, Joyce, Kodis, Orens, Parker, Roberson, Vomvoridis, Zaidman

New York University
Lawson, Weitzner

Northeastern University
Chan, Silevitch

Oak Ridge National Lab.
Fusion Energy Library, Lebouef, Meier, Mook

Physics International
Woo

Princeton Plasma Physics Lab
Chen, Cheng, Lee, Okuda, Tang, Graydon, Librarian

Lodestar Research Corp- Boulder
D'Ippolito, Myra

SAIC - Virginia
Drobot, Mankofsky, McBride, Smith

Sandia Labs, Albuquerque
Freeman, Poukey, Quintenz, Wright

Sandia Labs, Livermore
Marx, Wilson, Hsu

Stanford University
Blake, Buneman, Gledhill Physics Library

TRW
Wagner

Vista Research Inc.
Crystal

University of Arizona
Carlile

University of California, Berkeley
Arons, Birdsall, Chorin, Graves, Haller, Hess, Lichtenberg, Lieberman, McKee, Morse, Roth, Vahedi, Verboncoeur

University of California, Davis
DeGroot

University of California, Irvine
Rynn

University of California, Los Angeles
Abdou, Dawson, Decyk, Luhmann, Prinja

University of Illinois
Kushner

University of Iowa
Joyce, Knorr, Nicholson

University of Maryland
Guillory, Rowland, Winske

University of New Mexico
Anderson, Humphries

University of Pittsburgh
Zabusky

University of Southern California
Kuehl

University of Texas
Horton, McMahon, Tajima

University of Washington
Potter

University of Wisconsin
Emmert, Hershkovitz, Intrator, Scheur, Shohet

Varian Associates
Anderson, Grant, Helmer, Kenyon

Universität Innsbruck
Cap, Kuhn

I.N.P.E.
Alves, Bittencourt, Montes

University of Toronto
Stangeby

Riso National Laboratories
Lynov, Pecseli

Culham Laboratory
Eastwood

Imperial College
Burger

Oxford University
Allen, Edgley

Ecole Polytechnique, Palaiseau
Adam

Universite Paris
Raviart

IPP-KFA
Reiter

Max Planck Institute für Plasmaphysik
Biskamp, Chodura

University Bayreuth
Riemann, Schamel

Universität Kaiserslautern
Wick

Israel
Gell

Tel Aviv University
Cuperman

Hiroshima University
Tanaka

Kyoto University
Abe, Matsumoto, Jimbo

Nagoya University
Kamimura,Plasma Science Center, Research
Info. Center

Osaka University
Mima, Nishihara

Shizuoka University
Saeki

Tohoku University
Sato

University of Tromso
Armstrong, Trulsen

Centro de Electrodinâmica, Lisbon
Brinca

Ecole Polytechnique, Lausanne
Hollenstein